Optimal Fractional Order Proportional Integral Derivative Controller for Hydraulic Pitch Actuator of Wind Turbine Blade

MAHIDEREMARIAM ALEMU FEKREMARIAM

A Thesis Submitted to the Department of Electrical Power and Control Engineering

School of Electrical Engineering and Computing

Presented in Partial Fulfilment of the Requirement for the Degree of Master's in Electrical Power and Control Engineering (Control Engineering)

Office of Graduate Studies

Adama Science and Technology University

.

November 2022

Adama, Ethiopia

Optimal Fractional Order Proportional Integral Derivative Controller for Hydraulic Pitch Actuator of Wind Turbine Blade

Mahideremariam Alemu

Advisor: Dr. Endalew A.

A Thesis Submitted to the Department of Electrical Power and Control Engineering
School of Electrical Engineering and Computing
Presented in Partial Fulfilment of the Requirement for the Degree of Master's in Electrical Power and Control Engineering (Control Engineering)

Office of Graduate Studies
Adama Science and Technology University

November 2022
Adama, Ethiopia

DECLARATION

I hereby declare that this Master Thesis entitled "**Optimal Fractional Order Proportional Integral Derivative Controller for Hydraulic Pitch Actuator of Wind Turbine Blade**" is my original work. That is, it has not been submitted for the award of any academic degree, diploma, or certificate in any other university. All sources of materials that are used for this thesis have been duly acknowledged through citation.

Mahideremariam Alemu	______________________	________________
Name of student	Signature	Date

RECOMMENDATION

I the major advisor of this thesis, hereby certify that I have read the revised version of the thesis entitled **"Optimal Fractional Order Proportional Integral Derivative Controller for Hydraulic Pitch Actuator of Wind Turbine Blade"** which was prepared under my guidance by **Mahideremariam Alemu** Submitted in partial fulfillment of the requirements for the degree of Mater's of Science in Electrical Power and Control Engineering, postgraduate in Control Engineering. Therefore, I recommend the submission of the revised version of the thesis to the department following the applicable procedures.

Dr. Endalew Ayenew	____________________	________________
Major Advisor/Supervisor	Signature	Date

APPROVAL SHEET

I, the advisor of the thesis entitled **"Optimal Fractional Order Proportional Integral Derivative Controller for Hydraulic Pitch Actuator of Wind Turbine Blade"** and developed by **Mahideremariam Alemu,** hereby certify that the recommendation and suggestions made by the board of examiners are appropriately incorporated into the final version of the thesis.

Dr. Endalew Ayenew	____________________	________________
Major Advisor/Supervisor	Signature	Date

We, the undersigned, members of the Board of Examiners of the thesis by **Mahideremariam Alemu** have read and evaluated the thesis entitled **"Optimal Fractional Order Proportional Integral Derivative Controller for Hydraulic Pitch Actuator of Wind Turbine Blade"** and examined the candidate during the open defence. This is, therefore, to certify that the thesis is accepted for partial fulfillment of the requirement of the degree of Master of Science in Electrical Power and Control Engineering, postgraduate in Control Engineering.

____________________	____________________	________________
Chairperson	Signature	Date
Dr. Chala Merga		09.Nov.2022
External Examiner	Signature	Date
____________________	____________________	________________
Internal Examiner	Signature	Date

Finally, approval and acceptance of the thesis are contingent upon the submission of its final copy to the Office of Postgraduate Studies (OPGS) through the Department Graduate Council (DGC) and School Graduate Committee (SGC).

____________________	____________________	________________
Department Head	Signature	Date
____________________	____________________	________________
School Dean	Signature	Date
____________________	____________________	________________
Office of Postgraduate Studies Dean,	Signature	Date

ACKNOWLEDGEMENT

First and foremost, I would like to thank the Almighty God and His Mother, for keeping me, and giving me the strength to complete my study and in every step of my life.

I would like to express my heartfelt gratitude and indebtedness to Dr. Endalew Ayenew for the opportunity to work under his supervision and guidance. During this time, this research would not have been possible without his unending efforts, immense knowledge, deep patience, invaluable guidance, and answers to my numerous questions.

I would like to thank all my friends for their encouragement and understanding, their help, and lots of lovely memory with them can never be captured in words.

Finally, I would like to thank my family for their unlimited support and continuous encouragement in my studies. Also, I would like to deal special thanks to my father, Alemu Fekremariam who was the greatest inspiration for all my work until the end of his life on earth. Lastly, I would like to say "I have no words to talk about you but my father the God May your soul rest in peace in Heaven!"

'Thank you all!!!'

ABSTRACT

Due to the increase in power demand different electrical energy sources are considered in the world, wind energy is one of the renewable energy sources used to produce electrical energy based on the combination of a turbine and generator system. To improve the power production from wind energy larger turbine rotors are being built, which causes increased aerodynamics and other loads across the turbine blades, which results in a decrease in wind turbine efficiency and operating lifespan. The wind turbine blade pitch control system is a critical component for limiting mechanical overload on the overall system, as well as limiting the power of the turbine when the wind turbine is subjected to excessive wind speed. Therefore, this study develops an optimum controller for a hydraulic pitch angle actuator to control the wind turbine blade pitch angle and reduce loads on the blades when the system operates above rated wind speed. Bernoulli's equation and mass conservation laws apply to model the hydraulic turbine blade pitch actuator. Fractional order PID (FOPID) controller is used to improve the performance of the pitching mechanism and a genetic algorithm (GA) is used to find the optimal parameters of the controller based on minimizing integral absolute error (IAE) objective function. The overall system analysis and optimization were performed by using MATLAB/SIMULINK 2020a. The performance of the FOPID compared with the PID controller and the performance has been evaluated based on different reference signal-tracking capabilities. From the simulation result for the unit step input, the GA-FOPID controller gives a settling time of 0.1159sec, overshoot of 1.344%, and IAE of 0.010, the FOPID controller gives a settling time of 0.416 sec, overshoot of 13.427%, and IAE of 0.0351 and the GA-PID gives a settling time of 1.18 sec, overshoot of 29.74%, IAE of 0.1921. Similarly, the GA-FOPID maintains improved tracking performance by lowering the IAE value for both sinusoidal and staircase signals. When considering the effect of load torque at the blade root the GA-FOPID controller gives a settling time of 0.116 sec, and IAE of 0.01099, and the GA-PID controller gives a settling time of 1.188 sec, and an IAE of 0.1926. From the transient performance of the controller, the proposed GA-FOPID controller shows better performance than conventional PID. Lastly discuss the effect of turbine blade pitch angle change on tip speed ratio, rotor speed, mechanical power, and torque of wind turbine.

Keywords: Blade, Wind Turbine, Hydraulic Turbine Blade Pitch Actuator, Integral Absolute Error, GA-FOPID, GA-PID

TABLE OF CONTENTS

LIST OF FIGURE

LIST OF TABLE

LIST OF ACRONYMS

AC	Alternative current
CRB	Complex Root Boundary
DCV	Directional Control Valve
FOPID	Fractional Order Proportional Integral Derivative
GA	Genetic Algorithm
GA-FOPID	Genetic Algorithm Fractional Order Proportional Integral Derivative
GA-PID	Genetic Algorithm Proportional Integral Derivative
HAWT	Horizontal Axis Wind Turbine
ISE	Integral Square Error
IAE	Integral Absolute Error
ITAE	Integral Time Absolute Error
ITSE	Integral Time Square Error
IRB	Infinite Root Boundary
LVDT	Linear Variable Differential Transformer
MPPT	Maximum PowerPoint Tracking
MSE	Mean Square Error
PID	Proportional Integral Derivative
PI	Integral Derivative
RESs	Renewable Energy Source
RRB	Real Root Boundary
VAWT	Vertical Axis Wind Turbine
WECS	Wind Energy Conversion System
WT	Wind Turbine
WTG	Wind Turbine Generator

CHAPTER ONE

INTRODUCTION

1.1 Background

Energy availability is inextricably linked with long-term economic development. The vast majority of the world's commercial energy requirements are met by fossil fuels, which have negative environmental consequences (Studies et al., 2013). Many countries are increasingly adopting renewable energy sources to combat global warming and other environmental issues associated with these fossil fuels, also increased demand for electric energy is the other problem that leads the global society to consider renewable energy sources (Sahib & Nayl, 2019). Such energy sources are generally based on energy flows through the earth's ecosystem caused by solar insolation and geothermal energy (Gowdar & Mallikarjune Gowda, 2016).

Renewable energy sources have the potential to meet many times the current global energy demand. They have the potential to increase market diversity, secure long-term sustainable energy supplies, and reduce local and global atmospheric emissions. Renewable energy derived from renewable natural resources will contribute to long-term development (REN21, 2009).

Among the various renewable energy sources wind energy is one of the electrical energy sources, which contributes significantly to grid power installed capacity in the world and is emerging as one of the competing options for pollution reduction (Wu et al., 2019). Over the past 30 years, there has been a notable increase in the amount of electricity produced from wind energy. The cost of producing electricity from wind has fallen due to advancements in wind energy technologies (Islam et al., 2014). Up to 2021 Over 1800 TWh of electricity was obtained from wind energy, which accounts for more than 6% of global electricity and 2% of global energy. Globally additional 800GW wind power capacity was added in 2021 from the data around 100GW installed in China and the United States (Owusu & Asumadu-Sarkodie, 2016).

Wind energy is renewable and environmentally friendly, so systems for converting wind energy to electricity have grown rapidly (Gowdar & Mallikarjune Gowda, 2016). Every wind energy conversion system from simple units of generation to complex designs holds a turbine and generator, turbine is used to convert wind kinetic energy to mechanical energy then the generator is used to get electrical energy (Eltigani & Masri, 2015). Nowadays it become more complex because of the inclusion of different control systems to improve their ability to deal with wind variability while producing energy cost-effectively and reliably. And also because of the high dependency on climatic and environmental factors, control systems are required to ensure the efficient operation of WTs and the effective utilization of wind energy and to get maximum power (Apata & Oyedokun, 2020a)(Xue & Tai, 2012).

Most of the time the technology used to operate and control the angle of the blades in a wind turbine is known as pitch control, it is used to regulate the rotor speed by adjusting the angle of the wind turbines when the system is subjected to excessive wind variation. The pitch system is used to control how much energy the turbine's blades can extract and also helps to optimize the system's output power by adjusting the angle of the blades (Sahib & Nayl, 2019).

The wind turbine's pitch angle can be controlled collectively or individually, depending on the number of actuators in the nacelle of the wind energy generator, which is gaining popularity in wind turbine construction. Individual pitch angle control is achieved by driving wind turbine blades independently. In individual pitch angle control, the number of pitching mechanisms equals the number of blades of the wind turbine. But collective pitch angle control all blades are controlled at the same time using a single pitching mechanism (Gambier & Yunazwin Nazaruddin, 2018; Lasheen et al., 2016).

Figure 1.1 Blades action under pitch-controlled (Zhou & Liu, 2018)

The driving mechanism of wind turbine blade pitch angle is classified as hydraulic and electrical pitch control actuators. The electrical active pitch control system primarily employs a motor driving system to adjust the pitch angle of the wind turbine blade. On the other hand, the hydraulic pitch angle driving system employs a hydraulic actuation component to control the pitch angle of the wind energy generator. Both control actuators have their own set of characteristics (Dou et al., 2010). This study considers fractional-order proportional-integral-derivative control mechanisms for a large wind turbine's hydraulic pitch angle actuator.

1.2 Statement of the Problem

A wind energy conversion system is one of the electrical energy generating mechanisms based on the kinetic energy of wind. Due to the cubic relation between wind speed and the rotor power, when wind speed varies around the rotor the angular rotor speed and power also vary accordingly. When the system is subjected to excessive wind speed the turbine handles rotational speed above the allowable limit due to this the power output also increases above rated and it may cause damage to the mechanical component of the system. To reduce the effect of variation of wind speed around the blade of the turbine different turbine types use different techniques to protect the overall system from mechanical overload. Most of the studies consider controlling the rotor speed of wind turbines using the turbine rotor side converter. To reduce the effect of wind variation on turbine rotor output power add two independent controllers when the wind turbine operates in partial load and full load modes according to wind speed status. This causes the control system of wind turbines more complex and bulky. In variable-speed wind turbines, the turbine blade pitch control mechanism is used to reduce the effect of variation of output power and mechanical load on the turbine component due to the variation of wind speed. The effect of changing the pitch angle of the wind turbine blade affects the change of turbine tip speed ratio, rotor speed, rotor-developed torque, and rotor output power. The quality of the pitch driving mechanism is the basic consideration to reduce the system complexity and improve the efficiency of the turbine. One of the techniques used to change the pitch angle of the blade is the hydraulic wind turbine blade pitch actuator. Most studies take into account the electrical pitch angle actuator, which has a larger bandwidth, which is more desirable for faster actions such as individual pitching, but suffers from lower stiffness, faster transmission wear, greater backlash, less shock robustness, and higher power consumption. A hydraulic Pitch Actuator is used to overcome these drawbacks. It has higher stiffness, higher power-to-mass ratios, and large output torque. In addition, hydraulic pitch actuators are preferred for large to extreme aerodynamic loading situations because hydraulic systems are thought to be more fail-safe. This study considers the dynamic analysis and control of the hydraulic pitching mechanism of the wind turbine blade, it is modelled based on Bernoulli's equation and mass conservation laws. Then the performance of the actuator is improved using the FOPID controller.

1.3 The Objective of the Study

1.3.1 General Objective

The general objective of this study is to design an Optimal fractional order Proportional Integral Derivative Controller for a hydraulic pitch angle actuator of the blade wind turbine.

1.3.2 Specific Objective

- ✓ To develop the mathematical model of the hydraulic blade pitch actuator and mechanical system of a wind turbine.
- ✓ To design Proportional Integral Derivative (PID) and Fractional Order Proportional Integral Derivative (FOPID) controller techniques for hydraulic pitch actuators.
- ✓ To find the stability ranges for the parameters of both the PID and FOPID controllers
- ✓ To tune, the parameters of the controller using the Genetic Algorithm (GA) optimization technique to get the optimal parameter of the controllers.
- ✓ To show the tracking performance of the hydraulic system based on the different input reference signals using MATLAB/Simulink.
- ✓ To show the effect of the pitch angle change on wind turbine tip speed ratio, rotor speed, rotor-developed torque, and rotor output power.

1.4 Scope of the Study

This study considers developing the mathematical model for both wind turbine and hydraulic wind turbine blade pitch actuators. Then design Proportional-Integral Derivative and Fractional Order Proportional Integral Derivative Controller to improve actuator tracking performance by considering the effect of load torques at the root of blades introduced during system operation and obtain optimal parameters of the controller using a Genetic Algorithm. Lastly, perform the overall analysis of the control system on MATLAB/Simulink.

1.5 Limitations of the Study

This study restricted the simulation of the system using MATLAB/Simulink by demonstrating the interactions between the actuator's parts and the effect of turbine blade pitch angle change on the overall behavior of the turbine system. This is due to the difficulty of obtaining the necessary system components for the implementation of an existing device. Along with this, it requires the extra effort and expense required to create the prototypes of the actual implementation.

1.6 The Motivation for Study

Recently, there has been a lot of interest in producing power using various renewable energy sources (RESs). In particular, wind power is one of the most promising sources of energy in the world and it is expected to continue to grow quickly in the upcoming years. Wind speed fluctuations and variations in load demand provide significant challenges to wind energy conversion systems (WECS). From different types of wind turbines, horizontal axis wind turbines are the most efficient and commercially available type of wind energy conversion system. To reduce the predefined challenges most Modern horizontal axis wind turbines are built with a blade pitch control mechanism that is used to cover all operational wind speed areas. The blade pitch angle control mechanism is one of the protective methods to reduce the effect of mechanical overload when the wind speed is above the rated value. The effect of the pitch angle driving mechanism (actuator) on the overall system response is the basic thing that must be considered to improve the power quality of the system. To improve the overall system performance and the efficiency of the driving system apply different control mechanisms.

1.7 Significance of the study

Nowadays, Because of exceptional benefits such as global availability, low initial costs, environmental friendliness, and a rapid rate of technological development, there is a growing interest in using renewable energies today. Wind energy is the most accessible variable energy source and one of the most rapidly growing renewable energy systems. Furthermore, wind turbines play an important role as energy sources in microgrids and can be viewed as an alternative to a global network. Variable-speed wind turbine control systems are constantly evolving to provide more innovative and efficient solutions. The most important control technique used in a wind turbine to obtain the desired output power from the wind is blade pitch angle control. It is essential for turbine operation because it performs important actions like increasing energy capture, reducing operational load, and aerodynamic breaking. Enhancing energy capture entails improving the wind generation system's ability to regulate the voltage supplied from the system to the end user through optimal power harvesting. Another benefit of pitch angle control of wind turbine blades is that it adjusts the aerodynamic torque of the wind turbine when the wind speed exceeds the rated speed. To get effective operation and to improve the overall efficiency of the system needs a robust actuator to achieve the system's above-mentioned quality.

1.8 Organization of the study

The study has been organized into six chapters.

Chapter 1: Describes the background of the study, statement of problems, the objective of the study, scope, limitation, and significance of the study.

Chapter 2: Describes the literature review including the system's theoretical background, types of wind turbines, parts of the horizontal axis wind turbine system, wind turbine pitch angle actuator types, and related works on the control of wind turbine pitch angle actuators.

Chapter 3: Described the methodology follow during the development of the control system, a detailed derivation of the mathematical model of hydraulic pitch actuators and turbine system.

Chapter 4: Describes discussion on control techniques, stability ranges of the controller parameters, and optimization techniques used during the design of the control system to monitor the system properly.

Chapter 5: Describes the result of the system after simulation and includes a discussion based on the simulation result.

Chapter 6: Describes the overall conclusion and future work recommendation.

CHAPTER TWO

FUNDAMENTAL THEORIES AND LITERATURE REVIEW

2.1 Introduction

This section considers the basic classification of wind energy generation systems by considering their advantages and disadvantages, parts of the horizontal axis wind turbine, the power vs. wind speed relation effect in wind turbine operation, different wind turbine blade pitching techniques, and types of blade pitch actuators, and related works which consider improving the performance of wind turbine pitch angle actuator.

2.2 Types of wind turbines

Wind energy is a renewable energy that has drawn the interest of countries all over the world. Due to the system's applicability, there are various types of wind power generation systems. (Tan & Wang, 2013). The following diagram shows different types of wind energy generation techniques.

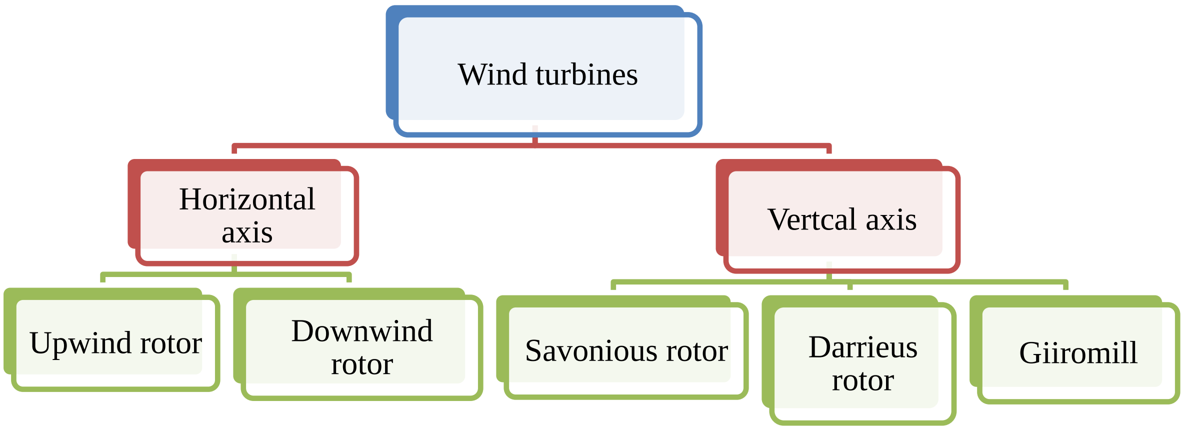

Figure 2.1 Classification of wind turbines

Wind turbines are classified into two types based on the installed axis of rotation.

I. Vertical axis wind turbines
II. Horizontal-axis wind turbines

Each type of wind turbine types has different parts. Especially the horizontal axis wind turbines have different types but most of the time it has almost the same number of subsystem. The following figure shows the basic sub-systems of horizontal-axis wind turbines. Figure 2.2 in this study mainly considers the turbine blade pitch angle subsystem and the effect of pitch angle change on the aerodynamic and mechanical performance of the wind turbine systems.

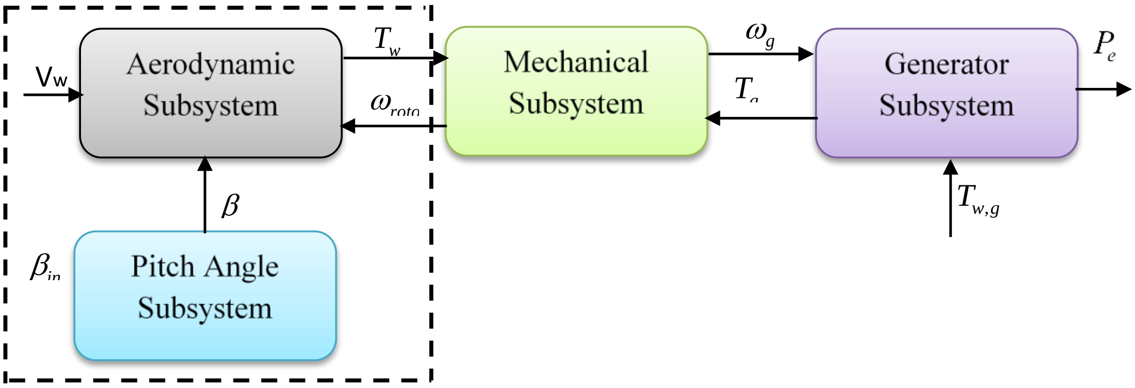

Figure 2.2 Main parts of horizontal axis wind turbines

I. Vertical axis wind turbines (VAWT)

A vertical axis wind turbine (VAWT) is a form of the wind turbine in which the rotor shaft is oriented transverse to the wind but not necessarily vertically, while the major components are located at the base of the turbine and blades are tapped at the top and bottom of a vertical rotor. The generator shaft is vertically oriented, with the blades pointing in the direction of the generator, which is placed on the ground or a short tower.

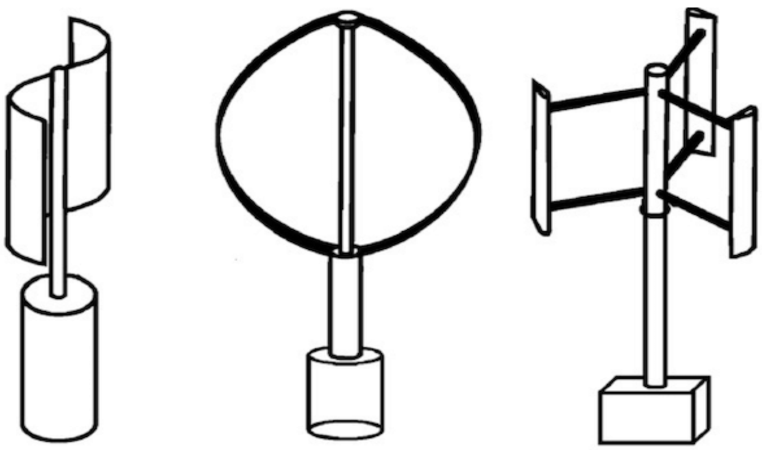

Figure 2.3 Different types of VAWT (Sunyoto et al., 2013)

Table 2.1 Advantages and Disadvantages of Vertical Axis Wind Turbines (VAWT) (Borg & Collu, 2012)

Advantages VAWT	**Disadvantages VAWT**
Wind from any direction can rotate the blade	The blades are close to the ground where the speeds are lower and have low output power
Low maintenance cost	Change in wind pressure and velocity causes stress on the system
Can be installed below the existing HAWT	Low starting torque
The nacelle component installed at the ground doesn't need a strong tower	Low swept area

II. Horizontal-axis wind turbines

The horizontal axis wind turbine (HAWT) is a commercial and efficient type of wind turbine. The axis of the rotor rotation in HAWT is parallel to the wind stream and the ground, and it uses a structurally strong tower because all of the wind turbine system components are positioned at the top of the tower.

It is categorized based on the number of fixed blades on the rotor and the position of the rotor.

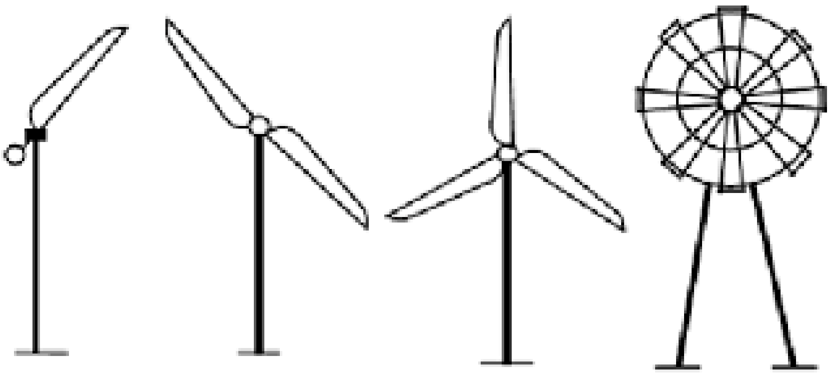

Figure 2.4 Types of HAWT (Kalpaktsoglou et al., 2019)

Based on the number of blades HAWT is classified as a One-bladed wind turbine, Two-bladed wind turbine, Three-bladed wind turbine, etc.

Table 2.2 Advantages and Disadvantages of Horizontal Axis Wind Turbines (HAWT) (Topologies, 2013)

Advantage of HAWT	**Disadvantage of HAWT**
High output power	Due to the size, it is difficult to transport, install, and maintenance
Can transform 40-50% of received wind energy into electricity	It harms the environment, especially the effect on wildlife and the local ecosystem.
High reliability	Strict regulations for installation
can operate at different wind speeds, it used to get optimal performance	To face the system toward wind direction it needs a complex yaw control system
Variable pitch is possibly used to adjust the angle of attack of the turbine	

2.3 Parts of Horizontal Axis Wind Turbine

The following are the components of the horizontal axis wind turbine and its functions (Baburajan & Ismail, 2017)

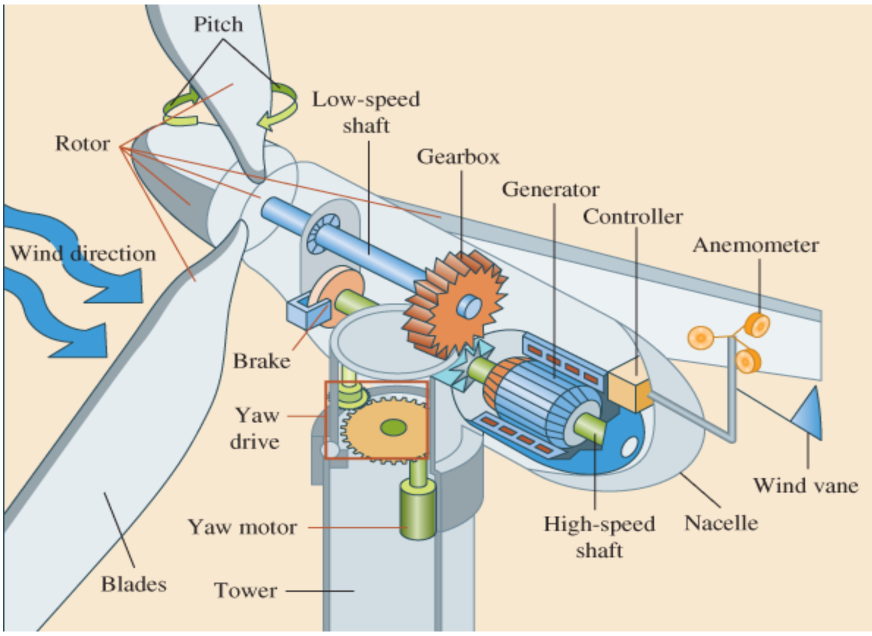

Figure 2.5 Part of Horizontal Axis Wind Turbine (Kalpaktsoglou et al., 2019)

- **Anemometer**: used to measure wind speed around the turbine rotor then sends the information to the control system.
- **Blades**: The major components to generate mechanical rotation of the rotor based on variable wind speed.
- **Brake**: is utilized to stop the rotor manually, electrically, or hydraulically when an emergency occurs.
- **Controller**: is a fundamental component of a wind energy generation system to regulate the general functioning of the overall system so that it may run under various operational circumstances and maintain favourable working conditions for the turbine system's parts.
- **Gearbox**: is located between the rotor and generator shaft, and is utilized as a transition between the low-speed shaft and the high-speed shaft. It is employed to achieve the speed needed by generators to produce power.
- **Nacelle**: a structure with a blade that can be seen at the top of a wind turbine tower. It includes the brake, controller, generator, and gearbox in addition to the shafts.
- **Pitch actuator and controller:** The wind energy generation system's pitch actuator and the controller are used to move the wind turbine's blades about their longitudinal axis, or in and out of the wind, respectively, to manage rotor speed and output power. The primary job of the pitch control system is to keep the rotor operating at its maximum capacity.
- **Rotor**: In the horizontal axis wind turbine is formed by the blades and the hub. It is located parallel to the direction of the wind flow.
- **Wind vane**: It is located at the top of the nacelle and detects changes in wind direction and interacts with the yaw drive to appropriately orient the turbine system to the direction of wind flow.
- **Yaw drive**: It keeps turbines facing the wind by orienting them to the direction of high wind flow measured by the wind vane. Different wind turbine systems employ various Yaw driving technologies.

2.4 Operating Condition of Horizontal Axis Wind Turbine

Especially horizontal axis Wind Turbine Generators operate in three modes: stop, partial load, and full load. Figure 2.6 depicts the relationship between generated output power and the operating range of wind speed. When the wind speed falls below cut-in speed, the WTG rotational speed is zero, and no power is generated since there is insufficient torque to rotate the wind turbine blade. The initial rotational speed of the turbine is called cut-in wind speed, which is typically between 3-4m/sec. If the wind speed is more than the cut-in value but less than the rated speed, the control system is used to extract the maximum power from the wind. This turbine operating range is known as maximum power point tracking (MPPT). The generator's power output is at its peak when the wind speed is between 12 and 17 m/sec. This is referred to as the rated power output, and the wind speed at which it is achieved is referred to as the rated speed. When the wind speed exceeds the rated value, the pitch angle control is activated to keep the generated output power constant at the rated value. In pitch angle control, the angle of the WTG blades is altered as a control variable for power management over the rated wind speed. (Sahib & Nayl, 2019) (Sohoni et al., 2016). As the wind speed exceeds the forces applied to the turbine structure increase accordingly, and there is a risk of damage to the rotor and other components of the wind energy generation system. As a result, a braking mechanism is used to stop the rotor. The cut-out speed is normally approximately 25m/sec.

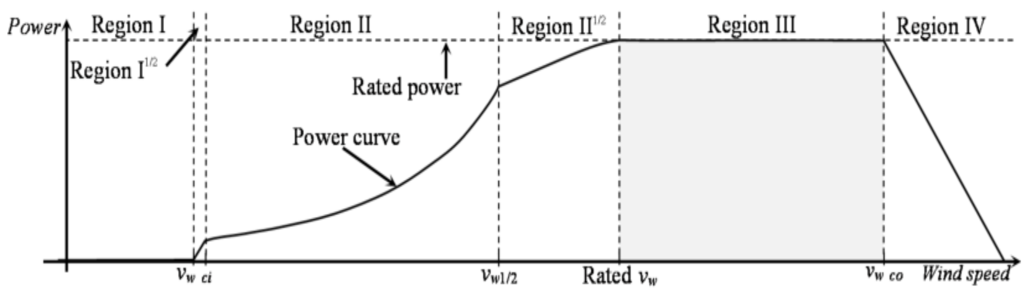

Figure 2.6 wind turbine power output variations with wind speed (Gambier, 2021)

2.5 Pitch Angle Control Techniques of Wind Turbine System

Different control systems can enhance the amount of wind energy captured by the turbine. Changing the angle of attack of the wind turbine blade is one of the control strategies used to increase power quality when wind speed is above the rated value (Pelin et al., 2018). There are three ways for controlling wind turbine blade pitch angle:

a) Passive stall control
b) Active stall control
c) Pitch control

a) Passive Stall Control

Passive stall control was employed in early wind turbine models. When the wind speed is less than the rated value, the blades can produce the greatest amount of power. However, when the wind speed exceeds the rated value, the strong wind creates turbulence at the back of the rotor blade, and reduced lifting force acting on the blade surface is used to reduce the rotational speed of the turbine. This is known as stalling. Wind turbine stalling is an effective strategy to regulate power output and prevent turbines from running away (Apata & Oyedokun, 2020a). The rotor blades of passive stall-controlled wind turbines are bolted to the hub at a fixed angle. The geometry of the rotor blade profiles is aerodynamically designed to create turbulence on the side of the rotor blade that is not facing the wind when the wind speed becomes too high.

b) Active stall control

It has an adjustable blade angle and a separate pitch controller (control mechanism) for each wind turbine blade. When the wind exceeds the rated value, the controlled blades turn more into the wind, resulting in the rejection of the controlled power. By altering the angle of attack of the blade when it is entirely turned into the wind, the captured power can be kept at the rated value. When the blade loses all interaction with the wind, causing the rotor stops. This operating situation can be employed when the wind exceeds the cut-out wind speed to stop the turbine and protect it from damage. Active stall control allows for keeping the power at the turbine design limit when the wind speed is above the rated value (Pelin et al., 2018)(Menezes et al., 2018).

c) Pitch control

The Pitch angle of variable-pitch wind turbines can be altered in conjunction with wind speed to maintain rated output power. The Pitch angle can be increased to lower the windward area of turbine blades at high wind speeds. Variable-pitch wind turbines are the greatest choice for large wind turbines because they can efficiently reduce blade stress, operates at all wind speed range, and enhance optimal power coefficient (Apata & Oyedokun, 2020).

To change a wind turbine's pitch angle, various actuators are employed. The common types of wind turbines' pitch angles actuators are:

1. Electrical wind turbine blade pitch actuator
2. Hydraulic wind turbine blade pitch actuator

1. **Electrical wind turbine blade pitch actuator**

The actuator, which is positioned at the blade's root, drives the blade when the system is operating at various wind speeds. One of the pitch angle actuators is the electrical one, which drives the system with an electric motor and gear. It has the advantages of compactness, good control precision, and high tracking performance, but it also has problems with erosion and less robustness against shocks.

2. **Hydraulic wind turbine blade pitch actuator**

An electro-hydraulic variable pitch angle actuator is the other technique to drive wind turbine blades. A hydraulic proportional valve, a hydraulic cylinder, and other parts are used to appropriately drive the system. Compared to the electrical pitch angle drive, the hydraulic actuator has superior qualities. To drive the megawatt wind turbine's blades using electrical actuators requires high motor torque to drive the system due to this it consumes above the usual or anticipated electric power. However, compared with an electric motor-based pitch angle actuation system, the electro-hydraulic control system has favourable qualities such as better power-to-mass ratios, good self-cooling ability, higher stability, higher stiffness, and large output torque (Lee & Moon, 2011).

2.6 Working Principle of Hydraulic Blade Pitch Actuator

A hydraulic variable pitch control system consists of a hydraulic pump, pilot-operated electro-hydraulic proportional directional control valves (DCV), a fluid tank, a liner-variable differential transformer (LVDT), a slider-crank mechanism, and a single rod double-acting hydraulic cylinder. A hydraulic cylinder located in the turbine's hub changes the blade pitch angle. The oil flow to and from the cylinders is controlled by valves, specifically a directional control valve.

The hydraulic cylinders piston road, which is attached to a crank connecting road mechanism, is the main engine of the independent hydraulic variable pitch control system. The displacement of the hydraulic cylinder piston rod and the pitch angle of the wind turbine are related, by modifying the position of the piston road of the cylinder's displacement can control the pitch angle of the wind turbine blade. It is accomplished by altering the electro-hydraulic proportional valve's control signal. Based on the difference between the actual blade pitch angle and the reference signals, the system controller generates a command signal to change the position of the proportional directional control valve spool. A hydraulic cylinder controls the direction and speed of the piston in response to the output hydraulic oil flow and direction from an electro-hydraulic proportional valve (Gu & Hui, 2008)(Qi, 2014).

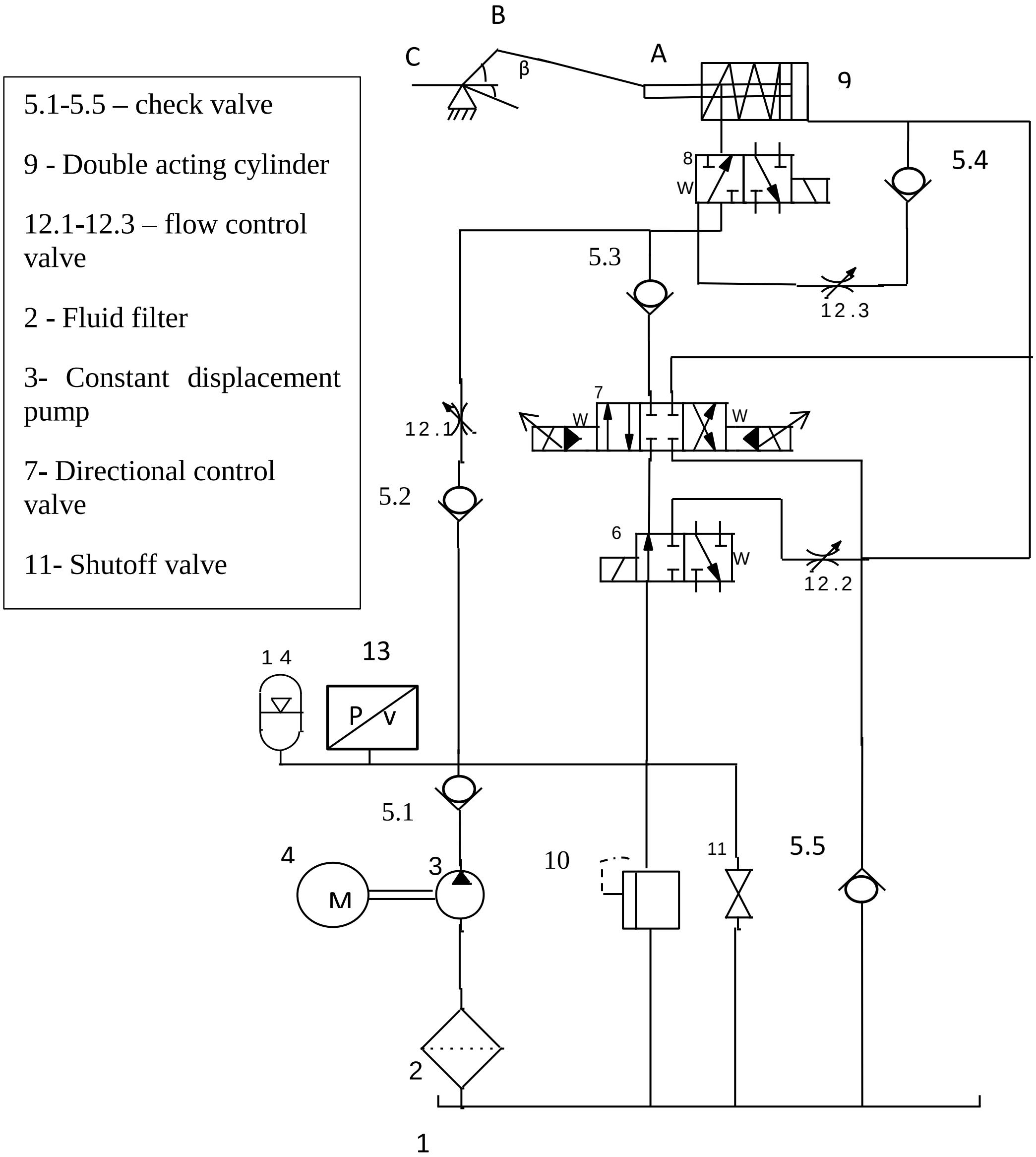

Figure 2.7 Simplified diagrams of the electro-hydraulic pitch angle actuator

Based on figure 2.7 the direction of the flow of liquid into and out of the terminal of the hydraulic cylinder decides the movement of the blade of the wind turbine. If the directional control valve is in the right position the fluid flow into the rod part of the hydraulic cylinder and removes without the rod cavity part of the hydraulic cylinder, in this case, the piston moves to the right position, and the pitch angle is reduced to 0^{o}. If the directional control valve moves to the left position the fluid flow into the without rod part of the cylinder and removes from the rod cavity of the hydraulic cylinder, in this case, the piston moves to the left position the pitch angle increases up to 90^o.

2.6 Components of Hydraulic Pitch Angle Actuator

2.6.1 Proportional Directional Control Valve (DCV)

Directional control valves (DCVs) are an essential component of hydraulic and pneumatic systems. It allows fluid to flow into multiple channels from one or more sources. DCVs are typically made up of a spool inside a cylinder that is mechanically or electrically actuated. The spool valve is classified based on several factors, including the number of lands and the number of ways the flow can enter and exit the valve. Every valve should have at least three ports: one for supply, one for return, and one for the load.

To reduce the power consumption and amplification to achieve high pressure and huge liquid flow of the directional control valve during operation using the pilot valve. A solenoid-operated pilot valve and a pilot-operated main valve comprise electro-hydraulic proportional valves. When a solenoid is activated, the pilot valve directs the flow to move the spool of the main valve, changing the direction and size of the flow in the hydraulic circuit. Pilot valves are crucial because they allow a small, manageable feed to control a much larger force. When the pilot valve is controlled by a solenoid, it is even more effective. A minimum oil pressure must be maintained in all operating conditions of the proportional control valve. In closed-loop control displacement force feedback is the operating mechanism of the electro-hydraulic proportional valve. The feedback spring connects the positioning of the main valve core and the pilot valve core. The upper cavity pressure of the main valve core will decrease as the electromagnet forces the pilot valve core down, overcoming the feedback spring's spring force. The main valve core moves open to ensure the proportional valve opens when the pressure differential is created. A feedback spring converts the main valve core's displacement into a force acting on the pilot valve core as feedback.

The valve is divided into three categories based on the alignment of the port opening with the land. An open-center or under-lapped valve is one in which the width of the land is less than the width of the port. The land width of a zero-lapped or critical-center valve matches the port width exactly. Closed-center or over-lapped valves have a land width that is bigger than the port width.

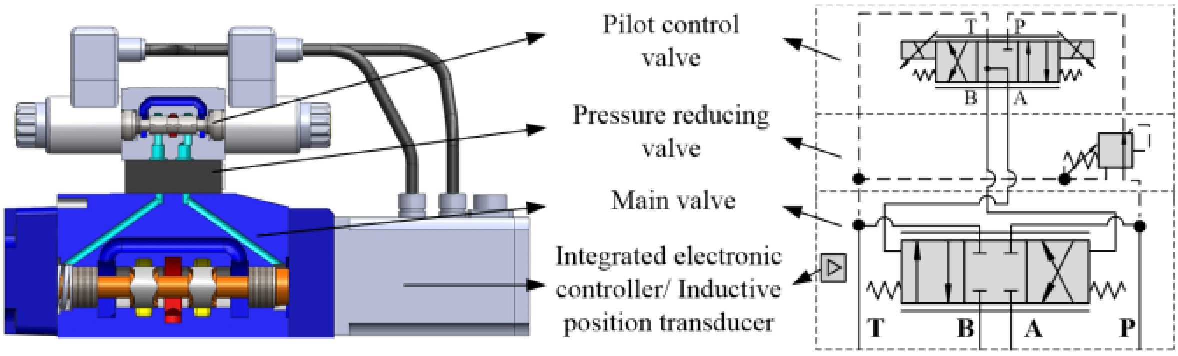

Figure 2.8 Diagrams for pilot-operated solenoid valve (Zhang et al., 2018)

The type of valve center may be related to the valve's flow characteristics. The majority of valves are made with a critical center because this allows for a direct correlation between the flow of the valve and the displacement of the spool. The proposed system uses the critical center valve. Due to the dead-band features in the flow gain, closed center valves are not appropriate. Dead band characteristics introduce a steady state inaccuracy and could result in backlash, which could cause stability issues in the control loop. Applications requiring an uninterrupted flow to maintain a reasonable fluid temperature and/or an increase in the hydraulic dampening are where open-center valves are used.

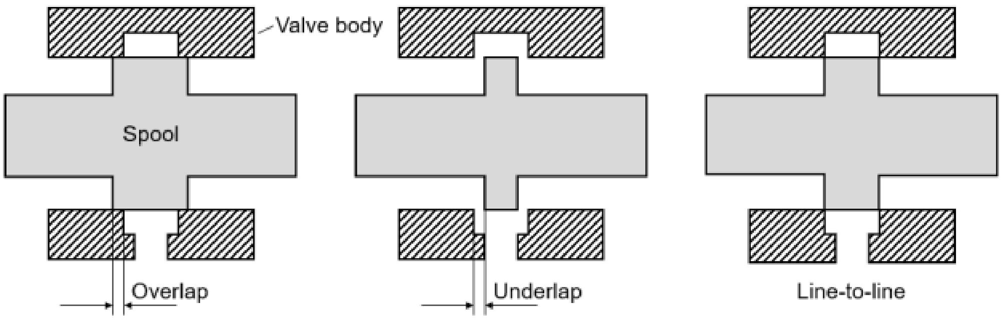

Figure 2.9 Different valve lapping when the spool is in a neutral position (Karlborg & Sten, 2021)

2.6.2 Types of Fluid Used in Hydraulic Systems

The type of fluid used to drive the hydraulic system must be specified because the various types of fluids used by hydraulic systems vary depending on the system's intended usage. The following section shows some of the fluid types used in hydraulic systems and their properties.

- **Petroleum-based hydraulic fluids:** These fluids are often utilized in any situation where there is a low risk of fire. This type of fluid provides many beneficial attributes, including excellent lubricity and cooling capacity, higher demulsibility, good oxidation resistance, higher viscosity index, good sealing characteristics, and ease of filtration cleaning. This sort of fluid has a flammability issue that makes it unsuitable for use in higher temperature conditions if there is a risk of fire.
- **Emulsions:** The capacity of oil to combine with water to produce an emulsion is defined as emulsibility. This fluid is classed as Water-in-oil and Oil-in-water.

✓ **Water-in-oil (inverse emulsion):** This emulsion contains more oil than water, and it is the most often used fire-resistant hydraulic fluid. It is made up of 40% water and 60% oil. It is combustible, lubricious, and has a high viscosity. The disadvantage of this type of fluid is that it has a low viscosity index due to the property of water and requires regular inspection since water may be removed from the system due to environmental effects. This sort of fluid application is in the mining industry.

✓ **Oil-in-water:** This emulsion includes water as the major phase and small oil droplets scattered in it, i.e. 5 percent oil and 95 percent water; as a result, it exhibits water properties. It falls under the category of flammable liquid. It also has low viscosity, which, due to the property of water, causes leakage, a loss in volumetric efficiency, and poor lubricating capabilities.

- **Synthetic hydraulic fluids**: This fluid type is made up of phosphate ester and fire-resistant fluid and is only suitable for high-temperature applications; it is not suitable for low-temperature applications. These types of fluids are man-made, they have certain hazardous qualities for the seal and surrounding materials. Its primary qualities include flammability, a high viscosity index, good viscosity, and lubrication. The problems associated with this sort of fluid are not natural and are not compatible with various environments.
- **Vegetable oil:** This sort of fluid is environmentally friendly, has good lubrication, has a moderate viscosity, and is less expensive. The issue is that it is less fire-resistant, has acidic properties, and oxidizes easily.

2.7 Previous work on pitch angle control

In a wind energy conversion system the power has cubic relation with wind speed, as wind speed fluctuates the output power also changes accordingly therefore different control techniques are used to get the desired output power to improve the performance of the system. Especially megawatt wind turbines blade have large rotational inertia due to this difficulty and challenge to control power fluctuations when wind speed is above the rated value. The pitch angle control is the technique used to regulate the output power when wind speed is above the rated value. Improving the performance of the system under the above-rated wind speed pitch angle control becomes one of the research focus areas (Tan & Wang, 2013).

Different control techniques are used to adjust the Pitch angle of the wind turbine and regulate the output power when it operates above rated wind speed. To control the blade pitch angle different techniques are considered (Sahoo et al., 2019)(Rashid & Halihal, 2019) the intelligent control techniques are used to control the pitch angle of the wind turbine. The hydraulic servo system driving mechanism which used to turn the turbine blade along its longitudinal axis. During the analysis of the hydraulic pitch actuator considered as a first-order system, this model doesn't show the exact dynamic property of the overall driving system. Most of the studies during modelling and simplification of the hydraulic driving systems considered first-order inertia. The input and the output variables are pitch angle and the time constant difference between the input variable and output variable this mathematical consideration neglects the actual characteristics of the driving system.

(Civelek et al., 2015) electrical servo actuator is used to drive the pitch angle of the wind turbine blade during modelling the motor 1^{st} order and the position control of the system consider a type 1 and 2^{nd} order system, lastly, all the parameters of the motor equals 1 for the simplicity of the computation. The dynamic behaviours of the blades both in pitch angle and pitch rate point are non-linear. In this study, these states are not considered, and pitch angle and blade dynamic behaviours are accepted as linear. The proper system modelling and parameter has a great effect on the performance measurement. In actuator operation consider the ideal operation of the system and Electric motor driven pitching systems have larger bandwidth, which is more desirable for faster actions such as individual pitching, however, suffering from smaller stiffness, quicker wear in transmission, and larger backlash. For large to extreme aerodynamic loading situations, hydraulic systems are considered more fail-safe.

(*Cho.s 2020*) Consider numerical modelling of hydraulic wind turbine blade pitch angle actuator for spar type floating wind turbine and its effect on the dynamic response of the turbine under the fault condition. During the investigation, the performance of the pitch angle actuator improves by using the proportional-integral (PI) controller and Ziegler-Nichols and Routh's methods used to get the value of the controller gain. During performance analysis consider square wave reference signal with maximum amplitude equals 15^{o}. From the result, the actuator introduces an overshoot and undershoot on the system output due to the change of reference signal, which highly affects the safe operation of the mechanical part of the system. In the study, the parameters of the controller tuned manually applying optimization techniques are used to improve the transient performance of the system and also reduce the computation time. In the study, the Performance analysis doesn’t consider the effect of the random variation of wind on the hydraulic pitch actuator.

(Wang & Chiang, 2016) consider two degrees of freedom hydraulic servo pitch angle control systems based on feedback linearization techniques. Two differential cylinders and an AC servo motor are the main components used to adjust the pitch of the wind turbine blade. The servo actuator most of the time considers the accuracy of the controlled parameter, it has a problem with the robustness of the system when the system is affected by disturbance. The number of hydraulic cylinder increase the complexity of the system and the hydraulic pump draws a high amount of power to drive the system.

(Meenu, 2019) consider fault-tolerant adaptive control technique for wind turbine blade pitch actuators and the performance of the controller measured based on the capability to regulate the output power for the system when the turbine operates under variable wind speed. The system analysis considers the effect of dynamic change in the pitch angle on the overall performance of the system. The result shows excessive overshoot in power output almost around two times the rated power, introducing High oscillation of output power and also high settling time. Due to this the control system introduces high mechanical overload and affects the overall performance of the system component.

From the above works of literature can be understood different studies consider different control techniques and different turbine blade pitch actuators. Each of them has its advantages and drawbacks to solve their drawbacks this study considers optimal fractional-order proportional-integral-derivative-based control mechanism to control the hydraulic blade pitch angle actuator. The performance of the overall system analyses is based on the tracking performance of different signals and also shows the dynamic effect of the hydraulic system on the overall operation of the wind turbine by considering variable wind speed.

CHAPTER THREE

METHODOLOGY AND SYSTEM DESCRIPTION

3.1 Introduction

The chapter considers detailed materials used during the study, the workflow block diagram of the study, the proposed system block diagram and its description, aerodynamic and pitch actuator modelling, and other elements of the system that contribute to achieving the goal.

3.2 Materials Used During the Study

To complete the entire analysis of the suggested control system for the thesis, MATLAB/SIMULINK is one of the working environments used. Math type and Microsoft Word 2016 are also used to complete the overall documentation.

3.3 Methods Used for the Study

To meet the result of the study with the above-mentioned objectives formal procedures will be followed.

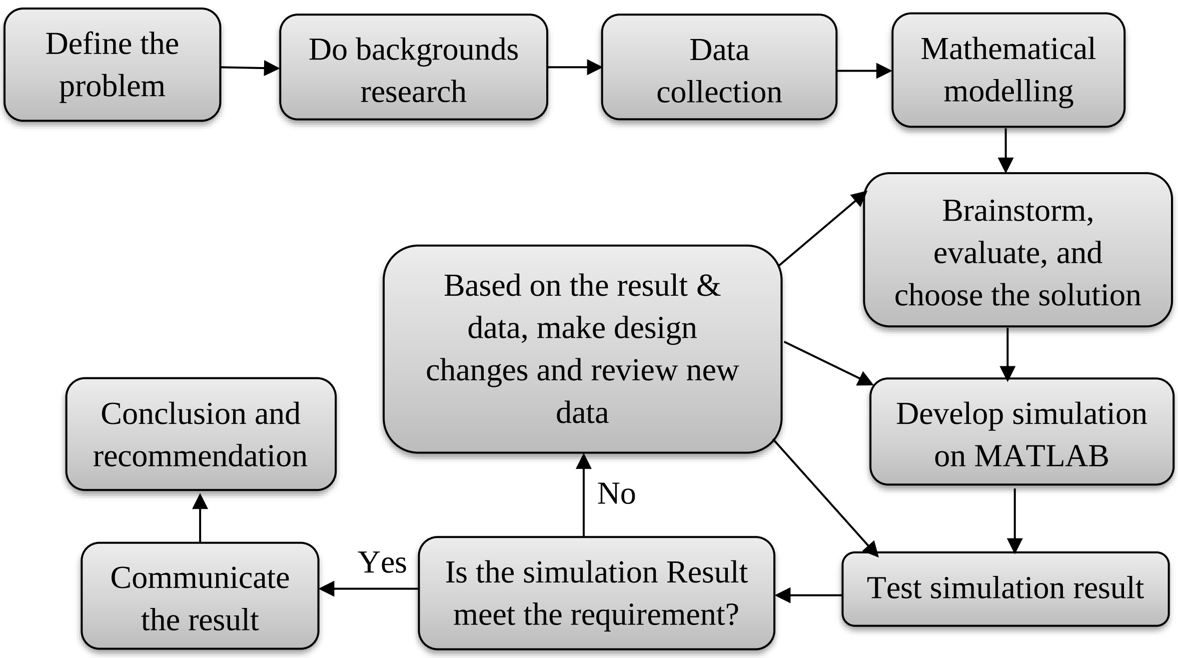

Figure 3.1 Workflow of the study

3.4 Description of the System Block Diagram

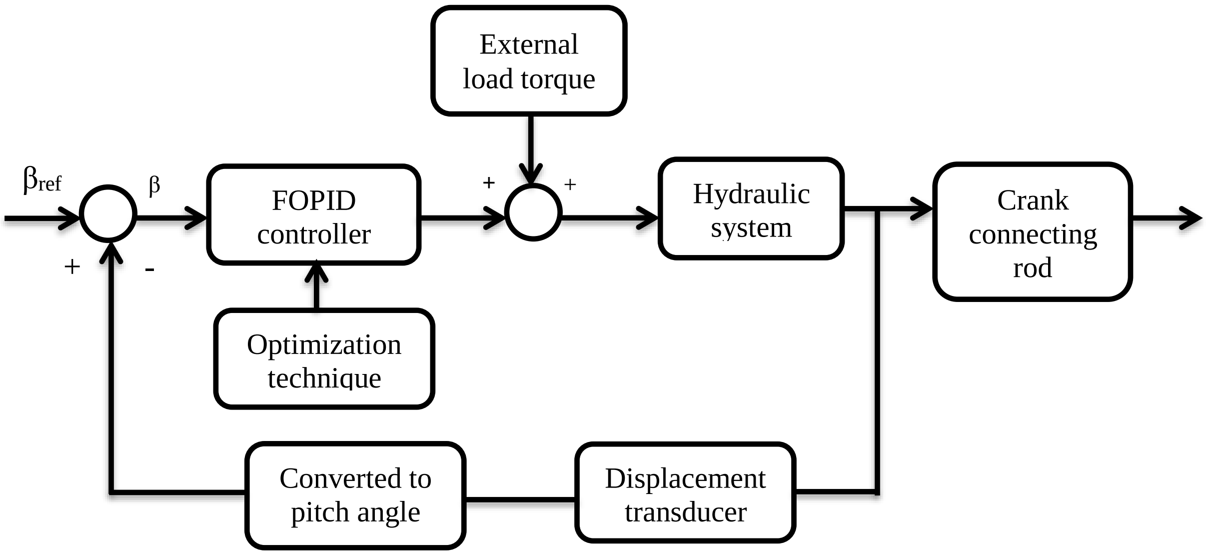

Figure 3.2 System block diagram

From figure 3.2 understand the basic component and working principle of the hydraulic wind turbine blade pitch angle actuator, the variable hydraulic pitch angle actuator controlled using GA-based fractional order proportional integral derivative controller. The error signal from the deviation of the actual pitch angle from its reference value is used to adjust the position and direction of the proportional directional control valve spool. The output of the proportional control valve is used to adjust the position and direction of the hydraulic cylinder piston and align the angle of the wind turbine blade to the reference angle because of the proportional relation between the change of displacement of the hydraulic piston and blade pitch angle. The change of the displacement of the piston is measured by the displacement transducer i.e. linear variable displacement transformer and feedback to the variable pitch actuator control system. Then the feedback pitch angle value is compared with a reference value and the deviation supply to the controller to adjust the control signal of a proportional control valve.

The external load considers the effect of the mass of external mechanical elements connected to the hydraulic cylinder piston and the force produced due to working with the surrounding environment like the turbulence nature of wind. External load torque cause to move the blade of the wind turbine without any changes in the command signal from the actuator system. To offset the load torque input an actuator control output signal is needed in the opposite direction.

3.5 Mathematical Modelling of Wind Turbine

The mathematical model of a wind turbine is critical to understand how it operates in its working environment and to improving its performance.

Let us consider the body with mass, m, and move under constant acceleration, a, the kinetic energy k_E by considering constant velocity, v, the same as the work done, w in moving that body starts from at rest and moves some distance, s, under the effect of the applied force F ,i.e.

$$k_E = w = Fs \tag{3. 1}$$

According to Newton's second law of motion, $F = ma$

Thus, the kinetic energy becomes

$$k_E = mas \tag{3. 2}$$

Based on the kinematics of the motion of the solid body, the velocity of solid body motion can be represented as:

$$v^2 = u^2 + 2as \tag{3. 3}$$

Where - u - Initial velocity of the body (m/sec) and v - Final velocity of the body (m/sec)

Based on the kinematic of the rigid body can drive the acceleration of an object

$$a = \frac{v^2 - u^2}{2s} \tag{3. 4}$$

Assuming the body starts to move from at rest, the initial velocity equals zero i.e. u=0,

$$a = \frac{v^2}{2s} \tag{3. 5}$$

Hence from equation (3.5), we have that

$$k_E = m(\frac{v^2}{2s})s \tag{3.5a}$$

$$k_E = \frac{1}{2} m v^2 \tag{3. 6}$$

Assume that the density of air does not vary with variation in altitude or temperature, Hence the kinetic energy (in joules) in the air of mass m moving with velocity v_w (wind) can be calculated from equation (3.6) above.

The power P of wind can be represented based on the rate of change of kinetic energy, i.e.

$$P = \frac{dk_E}{dt} = \frac{1}{2} \frac{dm}{dt} {v_w}^2 \tag{3. 7}$$

But mass flow rate $\frac{dm}{dt}$ can be represented as, $\frac{dm}{dt} = \rho_{air} A v_w{}^2$ where A is the area through which the wind is flowing and ρ_{air} is the density of air, and equation (3.7) becomes

$$P = \frac{1}{2}(\rho_{air} A v_w) v_w{}^2 \tag{3. 8}$$

$$P = \frac{1}{2}\rho_{air} A v_w{}^3 \tag{3. 9}$$

The actual mechanical power P_w which is extracted from the rotor blades (watts) can be obtained based on the difference between the upstream v_u and the downstream v_d wind powers.

$$P_w = \frac{1}{2}\rho_{air} A v_w (v_u{}^2 - v_d{}^2) \tag{3. 10}$$

Where v_u - Upstream wind velocity at the entrance of the rotor blades (m/sec), v_d - Downstream wind velocity at the exit of the rotor blades (m/sec)
Let

$$v_w = \frac{v_u + v_d}{2} \tag{3. 11}$$

v_w - Average wind velocities between the entry and exit of the rotor blades of the turbine.

The equation of mass flow rate become:

$$\rho_{air} A v_w = \frac{\rho_{air} A (v_u + v_d)}{2} \tag{3. 12}$$

Substitute the above two equations in the equation of actual mechanical power then

$$P_w = \frac{1}{2}\rho_{air} A (v_u{}^2 - v_d{}^2)\frac{(v_u + v_d)}{2} \tag{3. 13}$$

$$P_w = \frac{1}{2}(\rho_{air} A (\frac{v_u}{2}(v_u{}^2 - v_d{}^2) + \frac{v_d}{2}(v_u{}^2 - v_d{}^2))) \tag{3. 13a}$$

$$P_w = \frac{1}{2}(\rho_{air} A (\frac{v_u{}^3}{2} - \frac{v_u v_d{}^2}{2} + \frac{v_d v_u{}^2}{2} - \frac{v_d{}^3}{2})) \tag{3. 13b}$$

$$P_w = \frac{1}{2}(\rho_{air} A v_u{}^3 (\frac{1 - (\frac{v_d}{v_u})^2 + (\frac{v_d}{v_u}) - (\frac{v_d}{v_u})^3}{2})) \tag{3. 13c}$$

$$P_w = \frac{1}{2}\rho_{air} A v_u{}^3 C_p \tag{3. 14}$$

The power P_w can be defined as:

$$P_w = \frac{1}{2}\pi R^2 \rho_{air} v_w{}^3 C_p \tag{3. 15}$$

The relation between the captured wind power by the wind turbine and the available wind power around the rotor of the turbine is defined by the aerodynamic power coefficient C_p. This coefficient measures how effectively change wind energy into mechanical energy. It is also referred to as wind turbine rotor efficiency. The power coefficient is also known as the Betz limit after German physicist Albert Betz discovered it in 1919. The power coefficient is not a fixed value; it is related to the turbine tip speed ratio and turbine blade pitch angle in a nonlinear fashion (Azevedo, 2013). It can be defined as

$$Cp = \frac{power\ captured\ by\ the\ rotor}{power\ avaliable\ around\ the\ turbine\ rotor} \tag{3. 16}$$

Then based on the above relation the power coefficient is defined as:

$$C_p = \frac{1-(\frac{v_d}{v_u})^2 + (\frac{v_d}{v_u}) - (\frac{v_d}{v_u})^3}{2} \tag{3.16a}$$

$$C_p = \frac{(1-(\frac{v_d}{v_u})^2)(1+\frac{v_d}{v_u})}{2} \tag{3. 17}$$

Let λ_w represent the ratio of wind speed v_d downstream to wind speed v_u upstream of the turbine (Zhang et al., 2008), i.e.

$$\lambda_w = \frac{v_d}{v_u} \tag{3. 18}$$

The alternative representation of the tip speed ratio become

$$\lambda_w = \frac{speed\ at\ tip\ the\ blade}{wind\ speed} \tag{3. 19}$$

The tip speed ratio of the wind turbine is highly dependent on the rotational speed of the turbine and the length of the blades. The following represents the tip speed ratio of the wind turbine (Zhang et al., 2008), i.e.

$$\lambda_w = \frac{\omega_{rotor}\ \mathrm{R}}{\mathrm{v}_w} \tag{3. 20}$$

Where R - is the radius of the turbine (m), ω_{rotor} - is rotor speed (rad/sec)

By combining the two-equation the power coefficient become

$$C_p = \frac{(1+\lambda_w)(1-\lambda_w{}^2)}{2} \tag{3. 21}$$

The power coefficient is the main performance measuring quantity of the turbine system. It helps to get the maximum power extracted from wind energy. Differentiate C_p concerns λ_w and equate to zero to find the value λ_w that makes C_p a maximum

$$\frac{dC_p}{d\lambda_w} = \frac{d}{d\lambda_w}\left(\frac{(1+\lambda_w)(1-\lambda_w{}^2)}{2}\right) \tag{3.21a}$$

$$\frac{dC_p}{d\lambda_w} = \frac{1.(1-\lambda_w{}^2)+(-2\lambda_w)(1+\lambda_w)}{2} \tag{3.21b}$$

$$\lambda_w{}^2 + \frac{2}{3}\lambda_w - 3 = 0 \tag{3.21c}$$

$\lambda_w = 0$ or $\lambda_w = \frac{1}{3}$, the highest value λ_w used to get the maximum value of the power coefficient become $\lambda_w = \frac{1}{3}$

Substitute the selected value of the tip speed ratio in equation (3.21)

$$C_p = \frac{(1+\frac{1}{3})(1-(\frac{1}{3})^2)}{2} = \frac{16}{27}$$

The maximum value of the power coefficient is equal to $\frac{16}{27}$ the Betz limit says that no wind turbine can convert more than $\frac{16}{27}$ (59.3%) of the kinetic energy of the wind into mechanical energy turning a rotor, i.e. $C_{p\max} = 0.59 \text{ or } 59\%$. In real-world applications of the best-designed wind turbines, the Betz limit of 0.35 - 0.45 is common i.e. Wind turbines cannot operate at this maximum limit throughout their operational life.

The power coefficient is a non-linear function whose value is specific to each turbine type and is determined by the wind speed in which the turbine operates (Manyonge & Ochieng, 2014).

According to (Feng et al., 2021)(Melício et al., 2010) C_p is defined as a function of the tip speed ratio and the blade pitch angle β in degrees as

$$C_p(\lambda_w, \beta) = 0.73(\frac{151}{\lambda_i} + 0.58\beta - 0.002\beta^{2.14} - 13.2)e^{-18.4/\lambda_i} \tag{3. 22}$$

$$\lambda_i = \frac{1}{\lambda_w - 0.02\beta} - \frac{0.003}{\beta^3 + 1} \tag{3. 23}$$

The wind has a random variation in flow direction and speed. One of the key technologies considered in wind power generation systems to improve the stability of the generated power is power regulation. Mainly Three factors influence wind turbine output power: wind speed, pitch angle, and tip speed ratio. The aerodynamic power is directly proportional to the power coefficient of the wind turbine, which is affected by the blade tip speed and pitch angle. The graph below shows how the tip speed ratio affects power efficiency at various values of blade pitch angle.

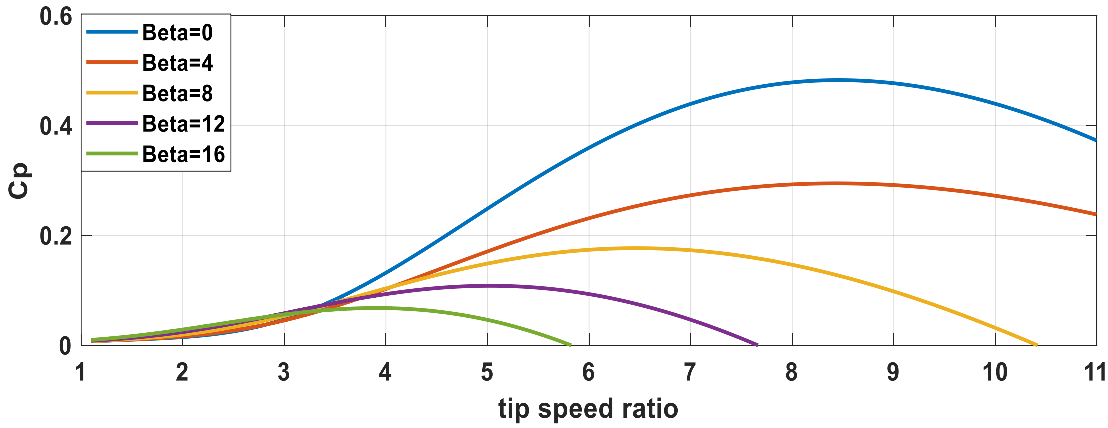

Figure 3.3 power coefficient vs. tip speed ratio graph

A variable-speed turbine can maintain the constant tip speed ratio required for the maximum power coefficient to be developed regardless of wind speed. To achieve the highest possible power coefficient, blade geometry is required. (Dong et al., 2022)(Rommel et al., 2020)

From the speed triangle the angle of relative wind for the rotor plane (φ) can be determined as;

$$\tan(\varphi) = \frac{(1-a)}{(1+a')}\frac{1}{\delta\lambda_w} \tag{3. 24}$$

a Axial interference factor and a' tangential interference factor are defined according to the blade aerodynamics.

δ - Non-dimensional blade radius defined by the different blade sections' from local (arbitrary) blade radius r and the maximum blade radius R, $\delta \in [0,1]$

$$\delta = \frac{r}{R} \tag{3. 25}$$

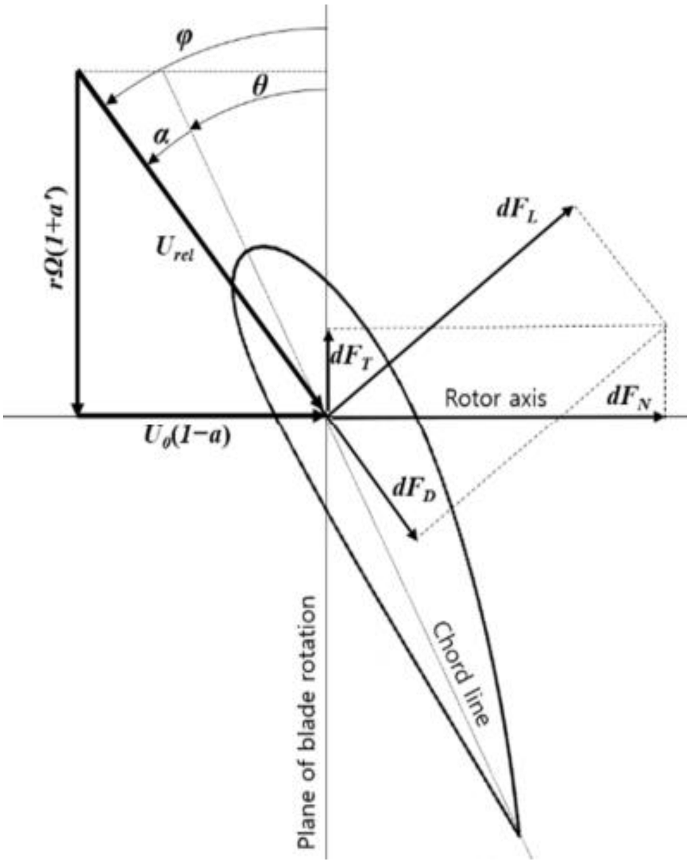

a - Axial interference factor

a' - Tangential interference factor

r - Section radius

α - Angle of attack

φ - In flow angle

θ - twist angle

$\omega_{rotor} = \Omega$ - Angular velocity of the rotor

U_{θ} - Free stream wind velocity

U_{rel} - Relative wind velocity

F_D - Drag force

F_L - Lift force

F_N - Normal force

F_T - Tangential force

Figure 3.4 Aerodynamic forces in wind turbine blade aerofoil and Wind speed triangle (Yang, 2020)

Based on the blade geometry the optimum operation to get an optimal amount of the tip speed ratio to improve the power coefficient for the rotor plane φ can be determined as:

$$\tan\varphi = \frac{1 - \frac{1}{3}}{\lambda_w \delta \left(1 + \frac{2}{9\lambda_w{}^2\delta^2}\right)} \tag{3. 26}$$

Substitute the equation of λ_w and δ solve the equation then we can get:

$$\tan\varphi = \frac{2R}{3r\lambda_w} \tag{3. 27}$$

$$\varphi = \tan^{-1}\frac{2R}{3r\lambda_w} \tag{3. 28}$$

θ The wind turbine blade twist angle at the tip of the wind turbine blade has a value range from 5 to 10^o. In this study, the twist angle around the blade of the horizontal axis wind turbine is around 7^o. (Johnson et al., 2016)(Burton et al., 2011)

From the relation between the blade's pitch angle and the angle of relative wind for the rotor plane the pitch angle can be represented as:

$$\beta = \varphi - \theta \tag{3. 29}$$

$$\beta = \tan^{-1} \frac{2R}{3r\lambda_w} - \theta \tag{3.29a}$$

$$\beta = \tan^{-1} \frac{2R}{3r(\frac{\omega_{rotor}\ \mathrm{R}}{\mathrm{v}_w})} - \theta \tag{3.29b}$$

$$\beta = \tan^{-1} \frac{2\mathrm{v}_w}{3r\omega_{rotor}} - \theta \tag{3. 30}$$

When r approches to R the rotor angular speed can be defined as:

$$\omega_{rotor} = \frac{2\mathrm{v}_w}{3R} \frac{1}{\tan^{-1}(\beta + \theta)} \tag{3. 31}$$

The mechanical torque developed by the wind turbine rotor that can drive an electric generator is formulated from equations (3.15) and (3.20).

$$T_w = \frac{1}{2} \rho_{air} \pi R^3 v_w{}^2 \frac{C_p}{\lambda_w} \tag{3. 32}$$

Table 3.1 Parameter for Wind Turbine (Azevedo, 2009)

Parameters	**Values**
1.5 MW Turbine Rotor	
No. of blades	3
Cut in speed (m/s)	3
Cut out speed (m/s)	25
Rated speed (m/s)	12
Optimal tip speed ratio	5.353
The maximum power conversion coefficient	0.48
Air density (kg/m^2)	1.225
Rated rotor speed (rpm)	16
Rotor radius (m)	38.0
Hub height (m)	70

3.6 Mathematical Model of Hydraulic Variable Pitch Control System

The directional control valve flow equation, the hydraulic cylinder flow equation, the hydraulic cylinder force balance equation, and the displacement equation of the crank connecting rod mechanism are all taken into account in the mathematical model of the hydraulic variable blade pitch angle actuator.

3.6.1 Force balance pilot-operated electro-hydraulic proportional valve

In proper operation of the directional control valve, the electromagnetic force and the spring force must be balanced. This relation can represent mathematically; (Olume et al., 2007)

$$F_i(s) = k_i i(s) \tag{3. 33}$$

$$F_f(s) = k_f x_v(s) \tag{3. 34}$$

Where F_i – proportional valve electromagnetic force, F_f – the pilot valve spring force, k_i –proportional valve electric current magnification factor, k_f -electromagnetic force magnification factor

From the above equations can get the following relation

$$k_i i(s) = k_f x_v(s) \tag{3. 35}$$

$$x_v(s) = \frac{k_i}{k_f} i(s) \tag{3.35a}$$

Therefore the current that controls the electromagnetic circuit become

$$i(s) = \frac{k_f}{k_i} x_v(s) \tag{3. 36}$$

3.6.2 Relationship between pitch angle and displacement of the cylinder

The displacement of the effective area of a hydraulic cylinder and the pitch angle of a wind turbine blade must be proportional, meaning that the wind turbine pitch angle varies with every change in the position of the piston. Based on figure 2.7 the pitch angle is 90° when the piston of the hydraulic cylinder is at the leftmost side. The pitch angle is zero degrees when the piston of the cylinder reaches the rightmost side. The permitted maximum pitch angle value is 90°, and the permitted lowest pitch angle is 0°. (Gu & Hui, 2008)(Olume et al., 2007)

To get the relation between piston position and blade pitch angle the system consists of the piston, liver, and crank connecting rod mechanism.

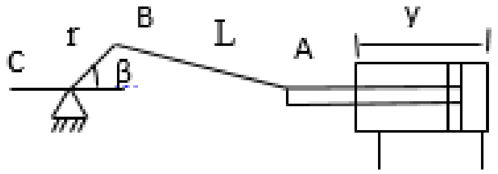

Figure 3.5 Single rods double-acting cylinder and change of blade pitch angle diagram

The relation of the position of the hydraulic cylinder piston between the blade pitch angle is obtained based on the triangle relation, completing the square and Pythagorean identity.

$$L^2 = r^2 + \Delta y^2 - 2r\Delta y\cos(\beta) \tag{3.37}$$

By rearranging the above equation the final relation can be represented as:

$$\Delta y = r(1-\cos(\beta)) + L(1-\sqrt{1-(\frac{r}{L}\sin(\beta))^2}) \tag{3. 37a}$$

The linear relationship between the pitch angle and piston position become:

$$y(s) = K_y\beta(s) \tag{3. 38}$$

Where- r – Length of the crank (m), y – Displacement of the cylinder (m), β – Pitch angle, K_y – cylinder displacement coefficient, L – length of link liver (m)

Let's take some points to get the linear relation between the change of pitch angle and the position of the hydraulic cylinder piston. The following table shows the relation between pitch angle and piston position based on some angles;

Table 3.2 Relation between Pitch angle (β^o) and Piston displacement y (m)

Pitch angle (β^o)	Piston displacement y (m)
0	0
π/9	0.0517
π/6	0.1143
π/4	0.2457
π/3	0.4243
π/2	0.72

Based on the relation between pitch angle and piston displacement the maximum and minimum value pitch angle and piston position become $\beta = [0, 90^o]$ and $y = [0, 0.72]$. From equation 3.38 the proportionality constant can be obtained:

$$K_y = \frac{y(s)}{\beta(s)}$$

$$K_y = \frac{y_{\max} - y_{\min}}{\beta_{\max} - \beta_{\min}}$$

$$K_y = \frac{0.72 - 0}{1.57 - 0} = 0.4585$$

Therefore the linear relation between pitch angle and piston displacement becomes:

$$y(s) = 0.4585\beta(s) \tag{3. 39a}$$

The above data set contains dependent or target variables (piston position) along with independent variables (pitch angle). The above models used predict the position of the hydraulic piston based on the variation of pitch angle. In this case, to check the error between the actual and the approximated relation between the change of pitch angle and piston displacement analysis based on the root mean square error.

Table 3.3 Validation of the relation between the actual and approximated Pitch angle (β^o) and Piston displacement y (m)

β^o	y_{actual} (m)	$y_{approximate}$ (m)	error	Squared error
0	0	0	0	0
π/9	0.0517	0.16	-0.1083	0.01172
π/6	0.1143	0.24	-0.1257	0.0158
π/4	0.2457	0.36	-0.1143	0.0130
π/3	0.4243	0.48	-0.0557	0.0031
π/2	0.72	0.72	0	0
			Total	0.04362

The mean square error becomes:

$$MSE = \frac{1}{n} \times \sum_{i=1}^{n} (y_{actual} - y_{approximate})^2 \tag{3. 40}$$

$$MSE = \frac{1}{6} \times (0.04362) \tag{3.40a}$$

$$MSE = 0.00727 \tag{3. 41}$$

From the above analysis, the mean square error between the actual and approximate value of the piston position is around 0.00727. Based on the value of mean square error the approximately linear relationship between pitch angle and hydraulic piston position has approximately zero error. Therefore the renaming part of the study works based on the approximate relation between the piston pitch angle and the hydraulic cylinder piston position.

3.6.3 Directional control valve characteristics and flow equation

The flow of fluid through the orifices of the directional control valve is the function of spool displacement and the output (load) pressure (Lei et al., 2010). Based on the operating principle of the directional control valve, when spool displacement x_v is taken as input and load flow Q_l is used as output, the flow equation of the directional control valve can be represented as (Lee & Moon, 2011) (Zhu & Jin, 2016)

$$Q_l = f(x_v, p_p) = C_d A_v x_v(s)\sqrt{\frac{2}{\rho}P_s - P_p} \tag{3. 42}$$

Where - C_d - Discharge coefficient, A_v – Cross-sectional area of the valve, ρ – hydraulic Fluid density, P_s – supply pressure, P_p –valve output pressure (load pressure)

The flow relationship for the control orifices is remarkably nonlinear to linearize using Taylor series expansion considering only the first part of the expansion equation high-order minor terms are eliminated because it has a smaller contribution to the output. The flow can be represented as (Ruderman, 2017)

$$\Delta Q_l = \left.\frac{\partial Q_l}{\partial x_v}\right|_{x_v=0} \Delta x_v + \left.\frac{\partial Q_l}{\partial P_p}\right|_{P_p=0} \Delta p_p \tag{3. 43}$$

From the flow equation of the directional control valve

$$\Delta Q_l = \left.\frac{\partial\left(C_d A_v x_v\sqrt{\frac{2}{\rho}P_s - P_p}\right)}{\partial x_v}\right|_{x_v=0} \Delta x_v + \left.\frac{\partial\left(C_d A_v x_v\sqrt{\frac{2}{\rho}P_s - P_p}\right)}{\partial P_p}\right|_{P_p=0} \Delta p_p \tag{3. 44 }$$

$$K_q = C_d A_v\sqrt{\frac{2}{\rho}P_s - P_p}, \text{ And} \tag{3.44a}$$

$$K_c = \frac{C_d A_v x_v \sqrt{\frac{2}{\rho} P_s - P_p}}{2(P_s - P_p)} \tag{3.44b}$$

From equation (3.33) the linearized flow equation can be represented as:

$$Q_l = K_q x_v - K_c P_p \tag{3. 45}$$

Where K_q - flow coefficient, K_c -flow pressure coefficient

3.6.4 The flow continuity equation of a hydraulic cylinder

The flow continuity principle is derived based on the concept of conservation of mass regardless of the complexity or direction of the flow and dimension of the pipe i.e. steady fluid flow through the conductor based on the concept of the mass of fluid flowing through any point in the conductor being the same. The flow is steady when the velocity at any period is constant. To approximately fulfill the conditions of steady flow, changes concerning time in temperature, fluid density, pressure, and flow rate must be almost zero.

Mathematically: (Li et al., 2015)

$$Q = A_1 v_1 = A_2 v_2 = \text{Constant} \tag{3. 46}$$

When considering our case the volumetric flow from the directional valve to the hydraulic cylinder can be represented as

$$Q_l = Q_s(t) + Q_h(t) \tag{3. 47}$$

Where Q_l - flow between the directional control valve and the actuator cylinder [m^3/s], Q_s - Flow covering the losses arising out of the liquid compressibility [m^3/s], Q_h - absorption of the actuator cylinder [m^3/s],

i. Absorption of the actuator cylinder: It means the flow of hydraulic fluid to drive the hydraulic cylinder piston. It can be expressed as:

$$Q_h(t) = A_c \frac{dy(t)}{dt} \tag{3. 48}$$

Where – A_c – active area of the hydraulic cylinder

ii. Liquid compressibility: It expresses the volumetric flow rate covering the loss arising out of the liquid compressibility. It can be expressed as

$$Q_s(t) = \frac{v_o}{4\beta_e} \frac{dP_p}{dt} \tag{3. 49}$$

Where β_e - Volume elastic modulus of hydraulic oil, v_o - Total volume of the cylinder

By combining the above two equations can get a volumetric flow rate between the distributor and actuator chambers:

$$Q_l = A_c \frac{dy}{dt} + \frac{v_o}{4\beta_e}\frac{dP_p}{dt} \tag{3. 50}$$

The Laplace equation of the above formula becomes:

$$Q_l(s) = A_c y(s)s + \frac{v_o}{4\beta_e} P_p(s)s \tag{3. 51}$$

3.6.5 Force balance equation of a hydraulic cylinder

Hydraulic components are unique in that it is often possible to offset or balance hydrostatic forces to reduce loads on lubricated surfaces. (Phan et al., 2021)

Generally the force balance equation of the system

$$F_p = F_v + T_{load} \tag{3. 52}$$

Where F_p – Force applied based on the surface of the hydraulic piston, F_v – Force applied from the piston area of the cylinder part, T_{load} - Load torque from blade root side

In our case to get the force balance equation of the hydraulic cylinder consider the fluid as an incompressible and frictionless rod for the pitch angle control. (Zhu et al., 2021)

$$P_p(t)A_c = M\frac{d^2y}{dt^2} + T_{load}(t) \tag{3. 53}$$

The Laplace transform of the above equation become:

$$A_c P_p(s) = My(s)s^2 + T_{load}(s) \tag{3. 54}$$

3.6.6 The transfer function of the system

The transfer function shows the relation between the input signal of the proportional control valve and the pitch angle of the wind turbine blade.

Based on equation (3. 54)

From the equation find P_p

$$P_p(s) = \frac{My(s)s^2 + T_{load}}{A_c} \tag{3. 55}$$

Substitute the value of P_p with the value of Q_l from equation (3. 45)

$$Q_l = k_q x_v(s) - k_c\left(\frac{My(s)s^2 + T_{load}(s)}{A_c}\right) \tag{3. 56}$$

Replace $x_v(s)$ by equation (3. 35)

$$Q_l = \frac{k_q A_c \, {}^{k_i}\!/_{k_f} \, i(s) - k_c M y(s) s^2 - k_c T_{load}(s)}{A_c} \tag{3. 57}$$

Replace $P_p(s)$ equation (3. 51)

$$Q_l(s) = \frac{A_c^{\,2} y(s)s + \frac{v_o}{4\beta_e} M y(s) s^3 + \frac{v_o}{4\beta_e} T_{load}(s)s}{A_c} \tag{3. 58}$$

Equate the equations (3.57) and (3. 58) and can get the following equation

$$y(s) = \frac{k_q A_c \, {}^{k_i}\!/_{k_f} \, i(s) - T_{load}(s)\left(\frac{v_o}{4\beta_e} s + k_c\right)}{\frac{v_o}{4\beta_e} M s^3 + k_c M s^2 + A_c^{\,2} s} \tag{3. 59}$$

$$y(s) = \frac{k_q \, {}^{k_i}\!/_{A_c k_f} \left(\frac{4\beta_e A_c^{\,2}}{v_o M}\right) i(s) - T_{load}(s)\left(\frac{1}{M} s + \frac{4\beta_e}{v_o M} k_c\right)}{s^3 + \frac{4\beta_e}{v_o} k_c s^2 + \frac{4\beta_e A_c^{\,2}}{v_o M} s} \tag{3. 60}$$

To get the simplified form take $\frac{4A_c^{\,2}\beta_e}{v_o M}$ as a common y(s) become

$$y(s) = \frac{4A_c^{\,2}\beta_e}{v_o M}\left(\frac{\frac{k_q k_i}{A_c k_f} i(s) - \frac{1}{A_c^{\,2}}\left(\frac{v_o}{4\beta_e} s + k_c\right) T_{load}(s)}{s\left(s^2 + k_c \frac{4\beta_e}{v_o} s + \frac{4A_c^{\,2}\beta_e}{v_o M}\right)}\right) \tag{3. 61}$$

The transfer function between the change of cylinder displacement and the control current becomes:

$$\frac{y(s)}{i(s)} = \frac{k_q k_i}{A_c k_f} \frac{\frac{4A_c^{\,2}\beta_e}{v_o M}}{s\left(s^2 + k_c \frac{4\beta_e}{v_o} s + \frac{4A_c^{\,2}\beta_e}{v_o M}\right)} \tag{3. 62}$$

$$\frac{y(s)}{i(s)} = \frac{k_q k_i}{A_c k_f} \frac{\omega_n^{\,2}}{s(s^2 + 2\xi\omega_n s + \omega_n^{\,2})} \tag{3.62a}$$

To get the relation between pitch angle and current use the relationship between pitch angle and change of cylinder displacement;

$$\frac{\beta(s)}{i(s)} = \frac{k_q k_i}{A_c k_f} \frac{\frac{4A_c^2 \beta_e}{v_o M}}{s(s^2 + k_c \frac{4\beta_e}{v_o} s + \frac{4A_c^2 \beta_e}{v_o M})} \frac{1}{k_y} \tag{3. 63}$$

$$\frac{\beta(s)}{i(s)} = \frac{k_q k_z}{A_c k_y} \frac{\omega_n^2}{s(s^2 + 2\xi\omega_n s + \omega_n^2)} \frac{1}{k_y} \tag{3.63a}$$

From the above equation, the natural frequency and damping coefficient can be defined as $\omega_n^2 = \frac{4A_c^2 \beta_e}{v_o M}$ the natural frequency becomes:

$$\omega_n = 2A_c \sqrt{\frac{\beta_e}{v_o M}} \tag{3. 64}$$

The damping coefficient of the system:

$$\xi = \frac{k_c}{A_c} \sqrt{\frac{\beta_e M}{v_o}} \tag{3. 65}$$

The transfer function between the pitch angle and the load torque becomes:

$$\frac{y(s)}{T_{load}(s)} = -\frac{1}{A_c^2} (\frac{v_o}{4\beta_e} s + k_c) \frac{\frac{4A_c^2 \beta_e}{v_o M}}{s(s^2 + k_c \frac{4\beta_e}{v_o} s + \frac{4A_c^2 \beta_e}{v_o M})} \tag{3. 66}$$

$$\frac{y(s)}{T_{load}(s)} = -\frac{1}{A_c^2} (\frac{v_o}{4\beta_e} s + k_c) \frac{\omega_n^2}{s(s^2 + 2\xi\omega_n s + \omega_n^2)} \tag{3.66a}$$

The relation with pitch angle can be represented as:

$$\frac{\beta(s)}{T_{load}(s)} = -\frac{1}{A_c^2} (\frac{v_o}{4\beta_e} s + k_c) \frac{\frac{4A_c^2 \beta_e}{v_o M}}{s(s^2 + k_c \frac{4\beta_e}{v_o} s + \frac{4A_c^2 \beta_e}{v_o M})} \frac{1}{k_y} \tag{3. 67}$$

Substituting values in Table 3.4 into (3. 63) and (3. 67), the overall open transfer functions of the system become:

1. between blade pitch angle and controls current is

$$\frac{\beta(s)}{i(s)} = \frac{23533.416}{s^3 + 8.6875 s^2 + 1077.8 s} \tag{3. 68}$$

2. between blades pitch angle and load torque is:

$$\frac{\beta(s)}{T_{load}(s)} = \frac{-4.362\times10^{-4}s - 0.0037}{s(s^2 + 8.687s + 1078)} \tag{3. 69}$$

Table 3.4 The parameters of the actuator of wind turbine (Olume et al., 2007)

Parameters	**Value**	**Units**
Length of crank (r)	0.48	m
Length of link lever (L)	0.6	m
Equivalent mass of the cylinder and load (M)	5000	Kg
Area of the rod-less chamber of a cylinder (A_c)	12.7*10^{-4}	m^2
The total volume of a cylinder (v_o)	8.38*10^{-4}	m^3
Effective bulk modulus (β_e)	7000*10^5	N/m^2
Gain of a linear differential transformer (k_s)	0.4	mA/mm
Magnification factor of electromagnetic force (k_f)	8.4	Nm/rad
Magnification factor of proportional valve current (k_i)	0.3	N/mA
Flow pressure amplification gain of a proportional valve (k_c)	0.026*10^{-10}	m^3/N.s
Flow amplification gain of the proportional valve (k_q)	0.356	m^2/s

The load torque depends on the effect of wind at the root of the wind turbine blade. It depends on the wind speed around the blade of the wind turbine and the value of the pitch angle of the blade. To get the aerodynamic torque effect at the hydraulic cylinder terminal use experiment based on the experimental data obtained from (Wang & Chiang, 2016)

CHAPTER FOUR

CONTROLLER DESIGN

4.1 Introduction

This chapter explains the proposed control techniques and stability analysis of the PID and FOPID controllers for wind turbine pitch angle actuator then discuss how to obtain the optimal controller parameters using the genetic algorithm optimization method.

4.2 PID Controller Design and Stability Analysis

Linear PID controllers are the most popular and widely used in different industries. PID controller can be interpreted as 'P' depends on 'present error,' 'I' depends on 'accumulated past error,' and 'D' depends on 'Future error'. The control signal applied to plant control input is the weighted sum of these three elements. The popularity and widespread use of PID or three-term controllers can be attributed primarily to their simplicity and performance characteristics, where the 'I' term ensures robust steady-state command tracking while the 'P' and 'D' terms provide stability and desirable transient behavior.

Proportional Integral Derivative control action is expressed as:

$$u(t) = K_p \; e(t) + K_i \int e(t)dt + K_d \frac{de(t)}{dt} \tag{4. 1}$$

Taking Laplace transforms

$$U(s) = \left[K_p + K_i \frac{1}{s} + K_d s \right] E(s) \tag{4. 2}$$

Table 4.1 Transient Property of PID Controller (Syed Hussien et al., 2015)

	Performance Effects			
	Rise Time	Settling Time	Overshoot	Steady-State Error
Proportional	Decrease	Small Change	Increase	Decrease
Integral	Decrease	Increase	Increase	Eliminate
Derivative	Small Change	Decrease	Decrease	Small Change

The closed-loop transfer function could be written as follows:

$$\frac{Y(s)}{U(s)} = \frac{G_c(s)G_p(s)}{1+G_c(s)G_p(s)} \tag{4. 3}$$

The GA optimization technique can be used in this project to select the PID controller parameters. Using fractional order controllers with non-integer derivation and integration parts is one method for improving PID controllers.

The Routh-Hurwitz criterion is an algebraic method for determining the absolute stability of a linear time-invariant system that is based on a control system characteristic equation with constant coefficients. The criterion evaluates whether or not any of the roots of the characteristic equation are located on the right-half s-plane. It also shows the number of roots on the $j\omega$ -axis and in the right half of the s-plane.

In this study, the Routh Hurwitz stability criteria were used to get the stability ranges of the PID controller parameters (Teixeira et al., 2007) (Yadav & Appan, 2016). To get the stability ranges of the parameters based on the statement of Routh criterion i.e. "Any system can be stable if and only if all the roots of the first column have the same sign, and if they do not have the same sign or if there is a significant change, then the number of sign changes in the first column equals the number of roots of the characteristic equation in the right half of the s-plane."

After substituting parameters in Table 3.4 into equation (3.69), the characteristic equation of the closed system from equation (4.3) becomes:

$$s^4 + 8.6875s^3 + (1078 + 23533.416K_d)s^2 + 23533.416K_p s + 23533.416K_i = 0 \tag{4. 4}$$

Table 4.2 Routh table for PID controller

s^4	1	$1078+23533.416K_d$	$23533.416K_i$	0
s^3	8.6875	$23533.416K_p$	0	0
s^2	a_1	a_2	0	0
s^1	b_1	0	0	0
s^0	c_1	0	0	0

From the system characteristic equation, the lower bound of the parameters can be determined, $K_p > 0,\ K_i > 0$ and $K_d > -0.0458$

In the third row of Table 4.2, for system stability the value a_1 is

The value of the Routh table become

$$a_1 = \frac{(8.687 \times (1077.8 + 23533.416K_d)) - 23533.416K_p}{8.687} \tag{4. 5}$$

$$a_1 = 1077.8 + 23533.416K_d - 2708.88K_p \tag{4. 5a}$$

Based on equation (4.5) the value of a_1 must have a positive value, therefore, considering the minimum value $a_1 = 0$, the relation between K_d and K_p is

$$K_p < 0.3978 + 8.687K_d \tag{4. 6}$$

From the 2nd column of table (4.2)

$$a_2 = \frac{23533.416K_i \times 8.687}{8.687} \tag{4. 7}$$

$$a_2 = 23533.416K_i \tag{4. 7a}$$

The fourth row of Table 4.2, b_1 must have a positive value for system stability and depends on the value of K_d and K_p

$$b_1 = \frac{(a_1 \times 23533.416K_p) - (a_2 \times 8.687)}{a_1} \tag{4. 8}$$

Substitute (4. 5) and (4. 7) into (4. 8) and after simplification can get

$$K_i < -311.8K_p{}^2 + 2708.88K_pK_d + 124.07K_p \tag{4. 9}$$

The last row of Table 4.2, c_1 must have always a positive value, to get a stable controller, therefore,

$$c_1 = \frac{b_1 \times a_2 - 0}{b_1} \tag{4. 10}$$

$$c_1 = a_2 = 23533.416K_i \tag{4.10a}$$

For system stability, $c_1 = a_2 > 0$ hence $K_i > 0$ is the lower limit. According to the above criteria, the lower bound of the controller parameters becomes $K_p > 0,\ K_i > 0$ and $K_d > -0.0458$, and the upper bound is free.

4.3 FOPID Controller Design and Stability Analysis

Podlubny proposed a general form of the PID controller, which is called the fractional order $PI^{\lambda}D^{\mu}$ controller, orders of integral (λ) and derivative (μ) actions have any real number values not only integer ones (Hui et al., 2019; Shutnan, 2018). The excess terms (λ and μ) provide flexibility to the control system, which is lacking in traditional PID controllers. Compared with the PID controller, the FOPID controller has additional two adjustable parameters, which makes the parameter tuning more flexible, it is the very important significance for improving the control accuracy, therefore, the fractional order $PI^{\lambda}D^{\mu}$ controller is applied in the hydraulic pitch angle drive system to improve the performance of the actuator.

The differential equation of the fractional order $PI^{\lambda}D^{\mu}$ controller is shown as an equation

$$u(t) = K_{pf}e(t) + K_{if}Dt^{-\lambda}e(t) + K_{df}Dt^{\mu}e(t) \tag{4. 11}$$

Applying the Laplace transform the transfer function of the controller can be expressed as:

$$G_c(s) = \frac{U(s)}{E(s)} = K_{pf} + \frac{K_{if}}{s^{\lambda}} + K_{df}s^{\mu} \tag{4. 12}$$

The orders of integral and differentiation are can be represented based on the relation between two axes. It can be seen that the conventional PID-type controllers are just a few specific points on the order planes. However, the orders of the controllers in fractional-order PID controllers can be relatively arbitrarily chosen. Normally, with stability considerations, $0 < \lambda, \mu < 2$ (Frp et al., 2019; Iru et al., 2018).

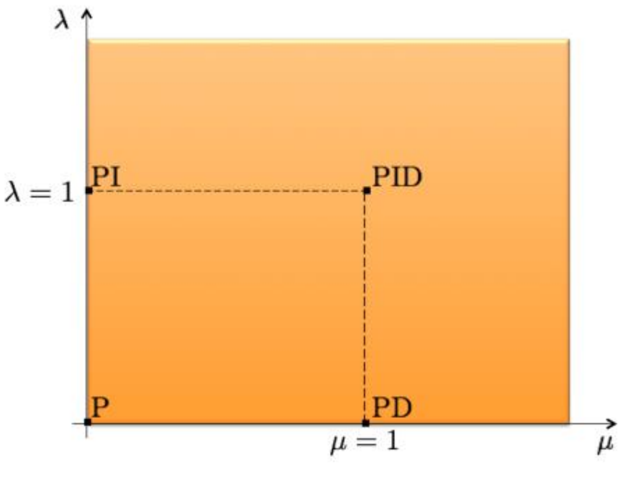

a. Control space of FOPID

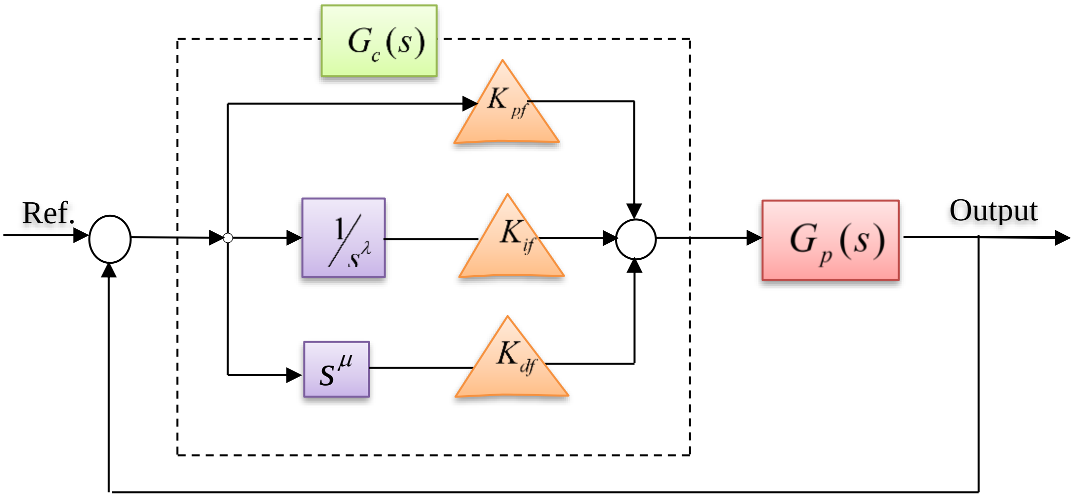

b. System block diagram

Figure 4.1 FOPID plane representation and block diagram (Chipipop & Calculus, 2019)

To get the stability ranges of fractional order controller parameters most of the time use an analytical method. During analysis Real Root Boundary (RRB), Complex Root Boundary (CRB), and Infinite Root Boundary (IRB) are the basic consideration used to get the global stability ranges of the fractional order dynamic system (Xu, 2018) (Hamamci, 2008)(Rhouma et al., 2021).

Let the system transfer function of the closed-loop system

$$y(s) = \frac{G_p(s)G_c(s)}{1+G_p(s)G_c(s)}u(s) \tag{4. 13}$$

Where - $G_c(s)$ - Transfer function of the controller and $G_p(s)$ - Transfer function of plant

Let the general representation of the transfer function of the plant represented as:

$$G_p(s) = \frac{N(s)}{D(s)} = \frac{b_n s^{\vartheta_n} + b_{n-1}s^{\vartheta_{n-1}} + ... + b_0 s^{\vartheta_0}}{a_n s^{\alpha_n} + a_{n-1}s^{\alpha_{n-1}} + ... + a_0 s^{\alpha_0}} = \frac{\sum_{i=0}^{n} b_i s^{\vartheta_i}}{\sum_{i=0}^{n} a_i s^{\alpha_i}} \tag{4. 14}$$

Where b_i and a_i are the coefficient of numerators and denominators of the plant transfer function and ϑ_i & α_i are the orders of the numerator and denominator of the plant transfer function.

The general transfer function of the fractional order controller

$$G_c(s) = \frac{U(s)}{E(s)} = K_{pf} + \frac{K_{if}}{s^{\lambda}} + K_{df}s^{\mu} \tag{4. 15}$$

From the closed loop equation in equation (4.13) the closed-loop characteristic equation of the overall system can be represented as:

$$P(s) = 1 + G_p(s)G_c(s) \tag{4. 16}$$

$$= 1 + \frac{b_n s^{\vartheta_n} + b_{n-1}s^{\vartheta_{n-1}} + ... + b_0 s^{\vartheta_0}}{a_n s^{\alpha_n} + a_{n-1}s^{\alpha_{n-1}} + ... + a_0 s^{\alpha_0}}(K_{pf} + \frac{K_{if}}{s^{\lambda}} + K_{df}s^{\mu}) \tag{4.16a}$$

$$\begin{aligned} &= s^{\lambda}(a_n s^{\alpha_n} + a_{n-1}s^{\alpha_{n-1}} + ... + a_0 s^{\alpha_0}) + (b_n s^{\vartheta_n} + b_{n-1}s^{\vartheta_{n-1}} \\ &\quad + ... + b_0 s^{\vartheta_0})(K_{pf} + K_{if}s^{\lambda} + K_{df}s^{\mu+\lambda}) \end{aligned} \tag{4.16b}$$

$$= \sum_{i=0}^{n}[a_i s^{(\alpha_i+\lambda)} + K_{df}b_i s^{(\vartheta_i+\lambda+\mu)} + K_{pf}b_i s^{(\vartheta_i+\lambda)} + K_{if}b_i s^{\vartheta_i}] \tag{4. 17}$$

Both the RRB, IRB, and CRB were obtained Based on the characteristic polynomial of the closed loop system.

To get the real root boundary substitute 0 in place of s term in the system characteristics equation. The closed loop characteristics equation has the RRB only if it holds the s^0 term, based on equation (4.16) generally the RRB of the system can be represented as:

$$\text{RRB line: } \begin{cases} K_{if} = 0 & for \quad s^{\vartheta_0} = 1, \vartheta_0 = 0 \\ None & for \quad s^{\vartheta_0} \neq 1, \vartheta_0 \neq 0 \end{cases} \tag{4. 18}$$

The IRB of the characteristic polynomial obtains by substituting $s = \infty$ in the equation (4.16). The IRB also depends on the order of the system. To determine the IRB of the system must consider three cases

Case I

If the system has equal order of pole and zero or the order of the derivative term of the controller is greater than the difference between the order of the pole and zero order of the system $k_d = 0$ is the value of IRB mathematically;

$$K_{df} = 0 \qquad for\ (\alpha_n = \vartheta_n)\ or\ (\alpha_n > \vartheta_n\ and\ \mu > \alpha_n - \vartheta_n) \tag{4. 19a}$$

Case II

If the order of the pole of the system is greater than the order of zero of the system and the order of the derivative term of the controller equals the difference value of the pole and zero of the system $K_{df} = {}^{-a_n}\!/_{b_n}$.

Mathematically:

$$K_{df} = {}^{-a_n}\!\!\diagup_{b_n} \quad for\ (\alpha_n > \vartheta_n\ and\ \mu = \alpha_n - \vartheta_n) \tag{4. 19b}$$

Case III

Both the above cases are not satisfied the control system $\alpha_n > \vartheta_n$ and $\mu < \alpha_n - \vartheta_n$ the system has no IRR.

To get the CRB of the system substitute $s = j\omega$ the characteristic equation of the closed loop of the system and find the boundary of the controller coefficient. Substitute $s = j\omega$ in the above characteristic equation (4.16),

$$P(\omega) = \sum_{i=0}^{n}[a_i(j\omega)^{(\alpha_i+\lambda)} + K_{df}b_i(j\omega)^{(\vartheta_i+\lambda+\mu)} + K_{pf}b_i(j\omega)^{(\vartheta_i+\lambda)} + K_{if}b_i(j\omega)^{\vartheta_i}] \tag{4. 20}$$

To solve the above equation, consider the following basic law for non-integer complex roots, $(\delta + j\omega)^{\varphi_p}$

$$(\delta + j\omega)^{\varphi_p} = (\delta^2 + \omega^2)^{\frac{\varphi_p}{2}}(\cos(\varphi_p \tan^{-1}(\frac{\omega}{\delta})) + j\sin(\varphi_p \tan^{-1}(\frac{\omega}{\delta}))) \tag{4. 21}$$

$$j^{\varphi_p} = \cos\varphi_p \frac{\pi}{2} + j\sin\varphi_p \frac{\pi}{2} \tag{4. 22}$$

Using (4. 21) and (4. 22), (4.20) is rewritten as

$$\begin{aligned} P(\omega) = \sum_{i=0}^{n}[(a_i(\omega)^{(\alpha_i+\lambda)}[\cos((\alpha_i+\lambda)\frac{\pi}{2}) + j\sin((\alpha_i+\lambda)\frac{\pi}{2})]) + (K_{df}b_i(\omega)^{(\vartheta_i+\lambda+\mu)} \\ [\cos((\vartheta_i+\lambda+\mu)\frac{\pi}{2}) + j\sin((\vartheta_i+\lambda+\mu)\frac{\pi}{2})]) + (K_{pf}b_i(\omega)^{(\vartheta_i+\lambda)}[\cos((\vartheta_i+\lambda)\frac{\pi}{2}) \\ + j\sin((\vartheta_i+\lambda)\frac{\pi}{2})]) + (K_{if}b_i(\omega)^{\vartheta_i}[\cos((\vartheta_i)\frac{\pi}{2}) + j\sin((\vartheta_i)\frac{\pi}{2})])] \end{aligned} \tag{4. 23}$$

When substituting $s = j\omega$ in the characteristic equation of the system holds both the imagery and real part.

From equation (4.23) the real part can be represented as:

$$\begin{aligned} \sum_{i=0}^{n} a_i(\omega)^{(\alpha_i+\lambda)}\cos((\alpha_i+\lambda)\frac{\pi}{2}) + K_{df}b_i(\omega)^{(\vartheta_i+\lambda+\mu)}\cos((\vartheta_i+\lambda+\mu)\frac{\pi}{2}) + \\ K_{pf}b_i(\omega)^{(\vartheta_i+\lambda)}\cos((\vartheta_i+\lambda)\frac{\pi}{2}) + K_{if}b_i(\omega)^{\vartheta_i}\cos((\vartheta_i)\frac{\pi}{2}) = 0 \end{aligned} \tag{4. 24}$$

From equation (4.23) the imaginary part can be represented as:

$$\sum_{i=0}^{n} a_i(\omega)^{(\alpha_i+\lambda)} \sin((\alpha_i+\lambda)\frac{\pi}{2}) + K_{df} b_i(\omega)^{(\vartheta_i+\lambda+\mu)} \sin((\vartheta_i+\lambda+\mu)\frac{\pi}{2}) + \\ K_{pf} b_i(\omega)^{(\vartheta_i+\lambda)} \sin((\vartheta_i+\lambda)\frac{\pi}{2}) + K_{if} b_i(\omega)^{\vartheta_i} \sin((\vartheta_i)\frac{\pi}{2}) = 0 \tag{4. 25}$$

Based on equations (4.24) and (4.25), the controller parameter can be computed where the value ω varies from 0 to ∞. (Hamamci, 2008)(Choudhary, 2015)

Take the value of K_{pf} and find the relation between K_{if} and K_{df} based on equations (4.24) and (4.25)

$$K_{if} = \frac{1}{\omega^{\mu+\lambda} \sin((\mu+\lambda)\frac{\pi}{2})} \frac{a_2(\omega)d_1(\omega) - a_1(\omega)d_2(\omega) + K_{pf}[c_2(\omega)d_1(\omega) - c_1(\omega)d_2(\omega)]}{b_1^2(\omega) + b_2^2(\omega)} \tag{4. 26}$$

$$K_{df} = \frac{1}{\omega^{\mu+\lambda} \sin((\mu+\lambda)\frac{\pi}{2})} \frac{a_1(\omega)b_2(\omega) - a_2(\omega)b_1(\omega) + K_{pf}[b_2(\omega)c_1(\omega) - b_1(\omega)c_2(\omega)]}{b_1^2(\omega) + b_2^2(\omega)} \tag{4. 27}$$

Take the value of K_{df} and find the relation between K_{pf} and K_{if} based on equations (4.24) and (4.25)

$$K_{pf} = \frac{1}{\omega^{\lambda} \sin(\lambda\frac{\pi}{2})} \frac{a_1(\omega)b_2(\omega) - a_2(\omega)b_1(\omega) + K_{df}[b_2(\omega)d_1(\omega) - b_1(\omega)d_2(\omega)]}{b_1^2(\omega) + b_2^2(\omega)} \tag{4. 28}$$

$$K_{if} = \frac{1}{\omega^{\lambda} \sin(\lambda\frac{\pi}{2})} \frac{a_2(\omega)c_1(\omega) - a_1(\omega)c_2(\omega) + K_{df}[c_1(\omega)d_2(\omega) - c_2(\omega)d_1(\omega)]}{b_1^2(\omega) + b_2^2(\omega)} \tag{4. 29}$$

Take the value of K_{if} and find the relation between K_{pf} and K_{df} based on equations (4.25) and (4.24)

$$K_{pf} = \frac{1}{\omega^{\mu+2\lambda} \sin(\mu\frac{\pi}{2})} \frac{a_2(\omega)d_1(\omega) - a_1(\omega)d_2(\omega) + K_{if}[b_2(\omega)d_1(\omega) - b_1(\omega)d_2(\omega)]}{b_1^2(\omega) + b_2^2(\omega)} \tag{4. 30}$$

$$K_{df} = \frac{1}{\omega^{\mu+2\lambda} \sin(\mu\frac{\pi}{2})} \frac{a_1(\omega)c_2(\omega) - a_2(\omega)c_1(\omega) + K_{if}[b_1(\omega)c_2(\omega) - b_2(\omega)c_1(\omega)]}{b_1^2(\omega) + b_2^2(\omega)} \tag{4. 31}$$

Where frequency-dependent variables $a_1(\omega), a_2(\omega), b_1(\omega), b_2(\omega), c_1(\omega), c_2(\omega), d_1(\omega), d_2(\omega)$ are as defined:

$$a_1(\omega) = \sum_{i=0}^{n} a_i(\omega)^{(\alpha_i+\lambda)} \cos((\alpha_i+\lambda)\frac{\pi}{2}),\ a_2(\omega) = \sum_{i=0}^{n} a_i(\omega)^{(\alpha_i+\lambda)} \sin((\alpha_i+\lambda)\frac{\pi}{2}) \tag{4. 32a}$$

$$b_1(\omega) = \sum_{i=0}^{n} b_i(\omega)^{\vartheta_i} \cos((\vartheta_i)\frac{\pi}{2}) \tag{4. 32b}$$

$$b_2(\omega)=\sum_{i=0}^{1} b_i(\omega)^{\vartheta_i}\sin((\vartheta_i)\frac{\pi}{2}) \qquad (4.\ 32c)$$

$$c_1(\omega)=\sum_{i=0}^{n} b_i(\omega)^{(\vartheta_i+\lambda)}\cos((\vartheta_i+\lambda)\frac{\pi}{2}) \qquad (4.\ 32d)$$

$$c_2(\omega)=\sum_{i=0}^{n} b_i(\omega)^{(\vartheta_i+\lambda)}\sin((\vartheta_i+\lambda)\frac{\pi}{2}) \qquad (4.\ 32e)$$

$$d_1(\omega)=\sum_{i=0}^{n} b_i(\omega)^{(\vartheta_i+\lambda+\mu)}\cos((\vartheta_i+\lambda+\mu)\frac{\pi}{2}) \qquad (4.\ 32f)$$

$$d_2(\omega)=\sum_{i=0}^{n} b_i(\omega)^{(\vartheta_i+\lambda+\mu)}\sin((\vartheta_i+\lambda+\mu)\frac{\pi}{2}) \qquad (4.\ 32g)$$

The general steps to find the stability range of the controller parameters are first to obtain the global stability ranges of the parameters of fractional order PID based on the RRB and IRB curve of the control system. The next step is to get the global stability range select order λ & μ that gives the biggest stability regions by plotting the CRB curves in (K_{pf}, K_{if}) the plane for some constant value of K_{df} (or in-plane for some constant value for K_{if}) by varying the value of λ and μ separately. The third step finds the stability range of the parameter of the controller by varying K_{pf}, K_{df} and K_{if} based on CRB curves.

To get the global stability region of the closed loop characteristic of the transfer function of the hydraulic actuator to become:

$$1+G_c(s)G_p(s)=1+(K_{pf}+\frac{K_{if}}{s^{\lambda}}+K_{df}s^{\mu})\times(\frac{23533.416}{s^3+8.6875s^2+1077.8s})$$

The system characteristic equation (4.16) becomes

$$s^{3+\lambda}+8.6875s^{2+\lambda}+1077.8s^{1+\lambda}+23533.416(K_{if}+K_{pf}s^{\lambda}+K_{df}s^{\mu+\lambda})=0$$

Based on equation (4.16) and system characteristic equation components can be related as

$$a_i s^{(\alpha_i+\lambda)}=s^{\lambda+3}+8.6875s^{\lambda+2}+1077.8s^{\lambda+1}$$

$$K_{df}b_i s^{(\vartheta_i+\lambda+\mu)}=23533.416K_{df}s^{\mu+\lambda}$$

$$K_{pf}b_i s^{(\vartheta_i+\lambda)}=23533.416K_{pf}s^{\lambda}$$

$$K_{if}b_i s^{\vartheta_i}=23533.416K_{if}$$

The RRB of the hydraulic actuator system, $\vartheta_i=0$,

$$K_{if}b_i=23533.416K_{if}$$

$$23533.416K_{if}=0,\ \mathrm{K}_{if}=0$$

For the hydraulic actuator system, there is no IRB, because the denominator order is greater than the order of the numerator i.e. $\alpha_n=3$ and $\vartheta_n=0,\ \alpha_n>\vartheta_n$ the order of derivative term of the controller found between $0<\mu<2$, therefore $\mu<\alpha_n-\vartheta_n$, *i.e.* $2<3$. Based on the above definition hydraulic actuator has no IRB curve.

The CRB of the hydraulic system:

$$(j\omega)^{\lambda+3}+8.6875(j\omega)^{\lambda+2}+1077.8(j\omega)^{\lambda+1}+23533.416K_{df}(j\omega)^{\mu+\lambda}+$$
$$23533.416K_{pf}(j\omega)^{\lambda}+23533.416K_{if}=0$$

Based on equation (4.23) the real and imaginary parts of the equation become:

$$\omega^{3+\lambda}\cos((3+\lambda)\frac{\pi}{2})+8.6875(\omega)^{2+\lambda}\cos((2+\lambda)\frac{\pi}{2})+1077.8(\omega)^{1+\lambda}\cos((1+\lambda)\frac{\pi}{2})+23533.416$$
$$K_{df}(\omega)^{\mu+\lambda}\cos((\mu+\lambda)\frac{\pi}{2})+23533.416K_{pf}(\omega)^{\lambda}\cos((\lambda)\frac{\pi}{2})+23533.416K_{if}=0$$

$$\omega^{3+\lambda}\sin((3+\lambda)\frac{\pi}{2})+8.6875(\omega)^{2+\lambda}\sin((2+\lambda)\frac{\pi}{2})+1077.8(\omega)^{1+\lambda}\sin((1+\lambda)\frac{\pi}{2})$$
$$+23533.416K_{df}(\omega)^{\mu+\lambda}\sin((\mu+\lambda)\frac{\pi}{2})+23533.416K_{pf}(\omega)^{\lambda}\sin((\lambda)\frac{\pi}{2})=0$$

The coefficients in equations (4.26) to (4.31) defined as

Let $a_1(\omega)=\omega^{(\lambda+3)}\cos((3+\lambda)\frac{\pi}{2})+8.86875\omega^{(2+\lambda)}\cos((2+\lambda)\frac{\pi}{2})+1077.8\omega^{(1+\lambda)}\cos((1+\lambda)\frac{\pi}{2})$

$$b_1=23533.416$$

$$c_1(\omega)=23533.416\omega^{\lambda}\cos((\lambda)\frac{\pi}{2})$$

$$d_1(\omega)=23533.416\omega^{\mu+\lambda}\cos((\mu+\lambda)\frac{\pi}{2})$$

$$a_2(\omega)=\omega^{(\lambda+3)}\sin((3+\lambda)\frac{\pi}{2})+8.86875\omega^{(2+\lambda)}\sin((2+\lambda)\frac{\pi}{2})+1077.8\omega^{(1+\lambda)}\sin((1+\lambda)\frac{\pi}{2})$$

$$b_2=0$$

$$c_2(\omega)=23533.416\omega^{\lambda}\sin((\lambda)\frac{\pi}{2})$$

$$d_2(\omega)=23533.416\omega^{\mu+\lambda}\sin((\mu+\lambda)\frac{\pi}{2})$$

Find the CRB of the system based on the relation between (K_{pf}, K_{df}) some fixed values of K_{if} which greater than 0, based on equations (4.30) and (4.31), and plot the graph of (K_{pf}, K_{df}) for $K_{if}=0$ and $K_{if}=150$ as shown in figure (4.2)

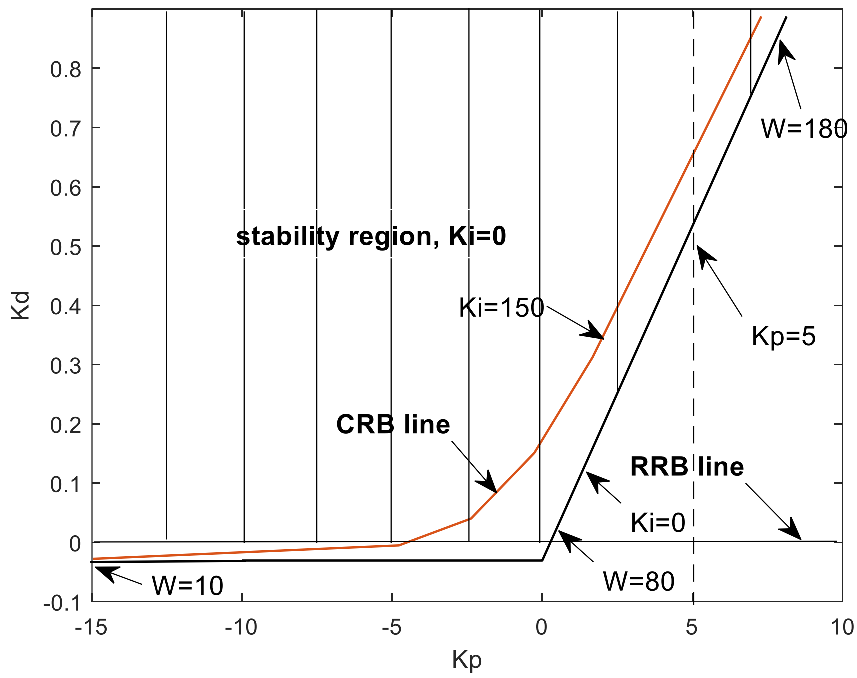

Figure 4.2 Stability region by varying K_{if} and $\lambda=\mu=1$

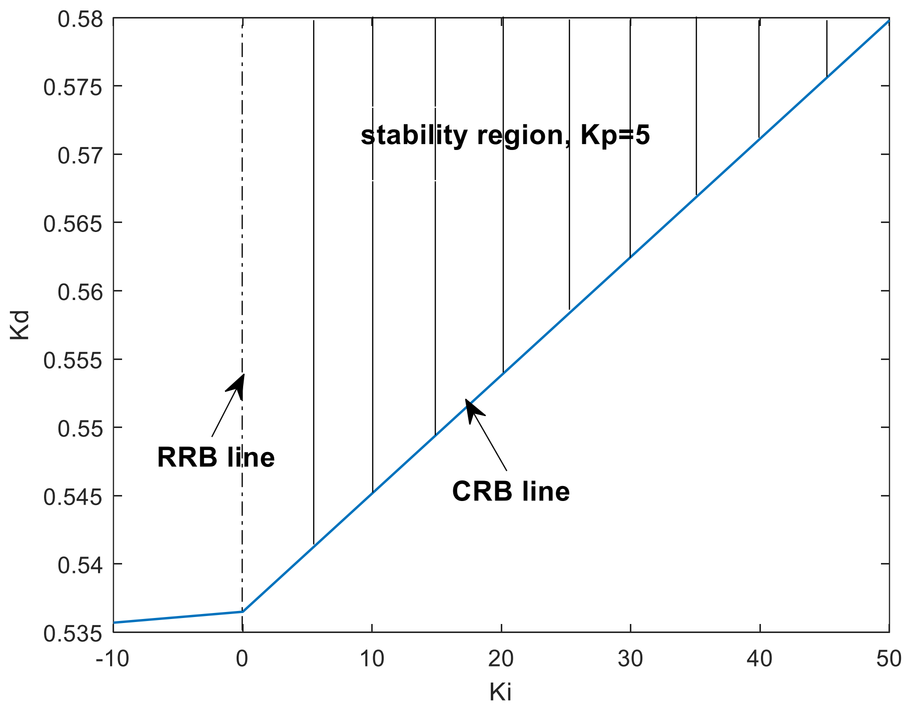

Figure 4.3 Stability region for $K_{pf}=5$ and $\lambda=\mu=1$

The fractional order controller parameter's upper stability ranges are decided based on the order of the derivative controller, from the IRB $\mu < 3$, i.e. the $\mu \in (0, 2)$ from the property K_{pf} *and* K_{df} have no maximum boundary which means the proportional and derivative parameters of the controller have the maximum stability range at infinity. From the RRB obtain $K_{if} = 0$, it is the minimum stability range of the integral component of the controller i.e. $K_{if} > 0$. The minimum ranges of the derivative and proportional and the upper bounds of an integral part of the controller are obtained based on the relation between the RRB, CRB, and IRB curve of the system.

The CRB curve depends on the boundary values of the parameters of the controller. In our case, the system has no IRB therefore the boundary K_{df} is at infinity but the system has RRB at $K_{if} = 0$. Figure (4.2) shows the relation of (K_{pf}, K_{df}) when the value of $K_{if} = 0$, any value of K_{if} found in the shaded region of the graph for example we can check the CRB curve when the value of $K_{if} = 150$ and also any value of K_{if} shifts the value of K_{pf} and K_{df} value to the positive direction. Based on the CRB graph in figure 4.2 the minimum interval of K_{pf} and K_{df} become zero.

If the sum of the value λ *and* μ equals zero the equation (4.26) and (4.27) denominator equals zero and the equation becomes undefined, therefore obtain the CRB curve relation (K_{if}, K_{df}) based on (K_{pf}, K_{df}) a curve by taking any two values of K_{if} and getting two CRB curves. Consider some fixed value K_{pf} from the relation planes (K_{pf}, K_{df}) and obtain two intersection points. Then based on the intersection points get the line equation i.e. $K_{df} = 0.000866K_{if} + 0.5365$, it helps to get the relation between (K_{if}, K_{df}) planes. Figure 4.3 shows the relation between (K_{if}, K_{df}) for fixed value of K_{pf}, let $K_{pf} = 5$, by changing the value of K_{pf} can obtain the stability range of the controller parameters.

The value λ *and* μ has a great effect on the width of stability regions of the controller parameters. To get the stability regions of the controller parameters change the value λ *and* μ between 0 and 2 separately. If μ greater than λ i.e. $\mu > \lambda$ based on the relation between (K_{pf}, K_{df}), $K_{if} = 0$ the system approaches infinity rapidly, which means that the system has greater stability region when $\mu > \lambda$.

Based on the graphical approach the stability range of the fractional order PID controller parameters is found in $K_{if} \in [0,\infty]$, $K_{pf} \in [-\infty,0]$ and $K_{df} \in [-\infty,0]$ or $K_{if} \in [0,\infty]$, $K_{pf} \in [0,\infty]$, and $K_{df} \in [0,\infty]$.

4.4 Genetic Algorithm Optimization

The Genetic Algorithm (GA) is a search-based optimization technique, it works based on the principles of Genetics and Natural Selection to produce the best results. GA solves the problem based on the process of generating a population of potential solutions. These solutions then go through recombination and mutation, giving birth to new children, and the process is repeated over and over. Each individual is assigned a fitness value based on the value of an objective function, and the fitter individuals have a better chance of mating and producing more "fitter" individuals. This is in line with the Darwinian Theory of "Survival of the Fittest" (West et al., 2016) (George & Ganesan, 2020).

This study considers GA to get the optimal parameter values of both PID and FOPID controllers. The genetic algorithm can search parallel population points, Due to this, it can obtain large and wide solution space search which helps to discover global optimum and avoid trapping to local optima.

4.4.1 Performance Indices

A performance index is a numerical evaluation of a system's performance that emphasizes key system variables. Different performance indices can be used to evaluate the overall performance of the control system. This proved the effectiveness of the controlled response by reducing the integral error until the process achieved the required set point. There are four common types of integral performance indices; Integral Absolute Error (IAE), Integral Square Error (ISE), Integral of Time Absolute Error (ITAE), and Integral of Time square Error (ITSE) (J.Jebakumar et al., 2014)

Integral Absolute Error (IAE)

$$IAE = \int_0^\infty |e(t)| dt \quad (4.33)$$

Different control systems use different integral performance indices based on the behavior of the control system. In this study consider IAE performance indices used to get the optimal value of both PID and FOPID controllers, because this performance measuring technique works on the absolute value of error without considering additional weighting, this helps to reduce the effect of the current value of error continuously and also able to reduce or eliminate the effect of the small error on the performance of the system. Additionally, IAE has the closest relationship to economic considerations.

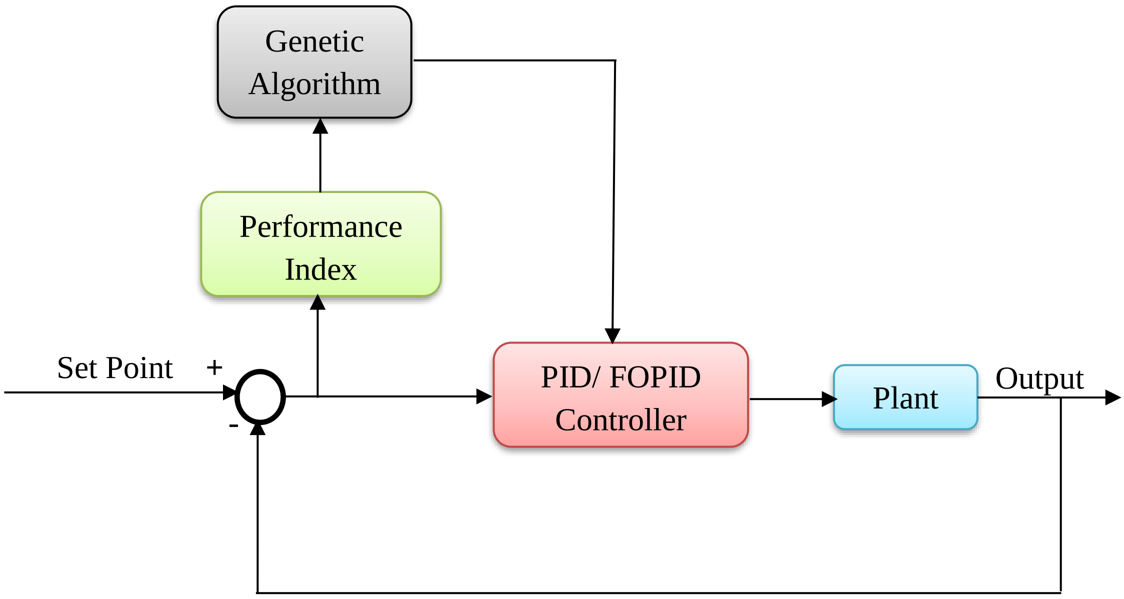

Figure 4.4 Block diagram of GA implementation

According to the system stability range of the parameters of the controllers discussed in the above section the optimal values of the gains of PID and FOPID controllers were obtained using a genetic algorithm. The response is gathered based on the minimization of the IAE performance index shown in equation (4.33). The range of parameters used during optimization is shown in the table below.

Table 4.3 Controller’s parameter for GA optimization

Parameter	**For GA-PID**	**For GA-FOPID**
Maximum generation	50	50
Population size	20	20
No. of parameters	3	5
Lower bound	[K_p K_i K_d] [0.001 0.001 -0.0458]	[K_{pf} K_{if} K_{df} λ μ] [0.00001 0.00001 0.00001 0.01 0.01]
Upper bound	[K_p K_i K_d] [10 10 5]	[K_{pf} K_{if} K_{df} λ μ] [25 10 10 2 2]

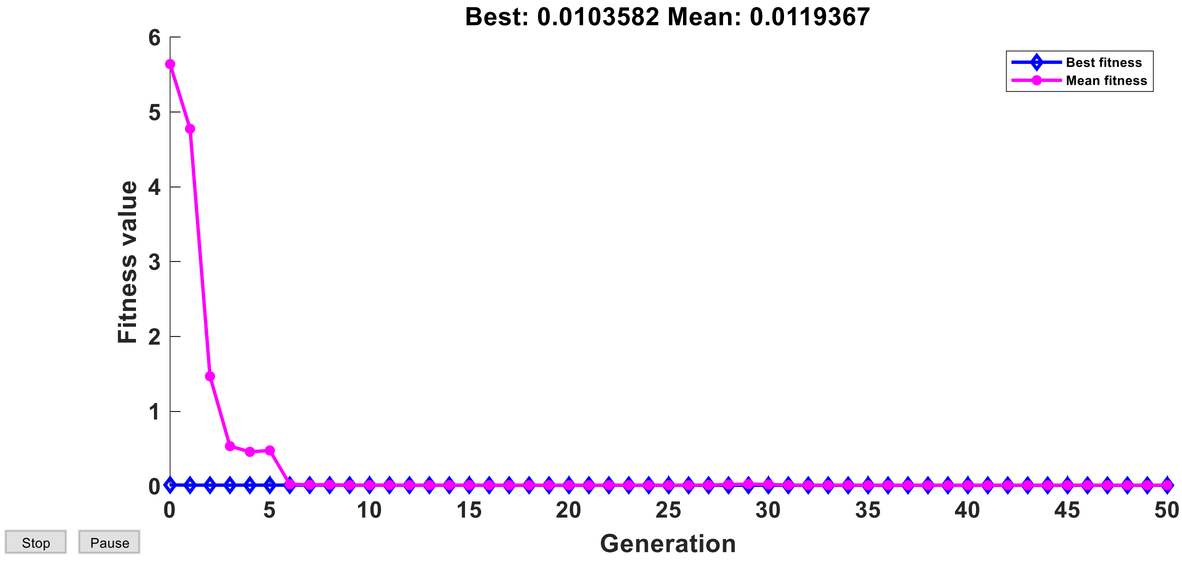

Figure 4.5 GA generation vs. fitness value graph for FOPID

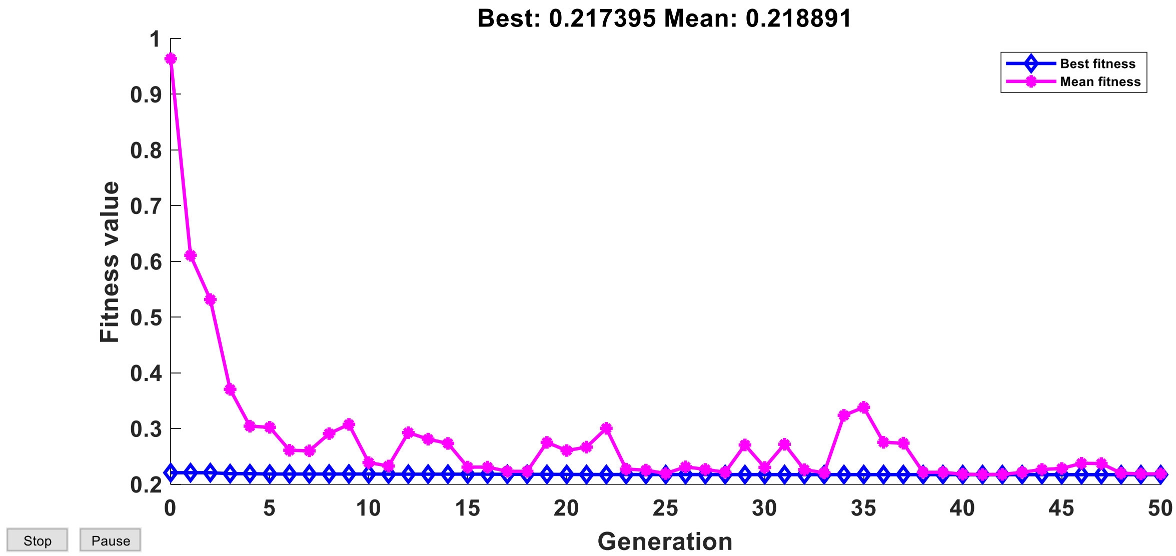

Figure 4.6 GA generation vs. fitness value graph for PID

The genetic algorithm is used to select the optimal controller gain between the upper and lower bounds. The optimum value of the controller's parameters is shown in the table below.

Table 4.4 Optimal parameters for PID and FOPID

Controller parameters	K_p	K_i	K_d	λ	μ
GA-PID	0.2928	1.7688	0.0013	--	--
GA-FOPID	12.8401	3.4142	0.5672	0.0680	1.6776

The graphical result from GA optimization with the best fitness value and mean value are shown below. From the optimization result graph, the best fitness value for GA-PID equals 0.2174 and the best fitness value for GA-FOPID equals 0.01035.

CHAPTER FIVE

RESULT AND DISCUSSION

5.1 Introduction

This chapter considers simulation and performance analysis of hydraulic pitch angle actuators for wind turbines and their performance effect on turbine mechanical dynamics. The simulation result and discussion consider the performance comparison between the proposed control systems with different control mechanisms based on the transient response to fulfill the objective of the study. The overall simulation is performed using MATLAB/SIMULINK. The complete system diagram is presented in Figure 5.1. It is a logically connected model of the rotor output power of the wind turbine, (3.15), the tip speed ratio of the wind turbine, (3.20), the power conversion coefficient of the wind turbine, (3.22), rotor speed of the wind turbine, (3.31), rotor output torque of wind turbine, (3.32), model of the actuator of the wind turbine blade, (3.68) and (3. 69), and the controller which is designed in chapter four.

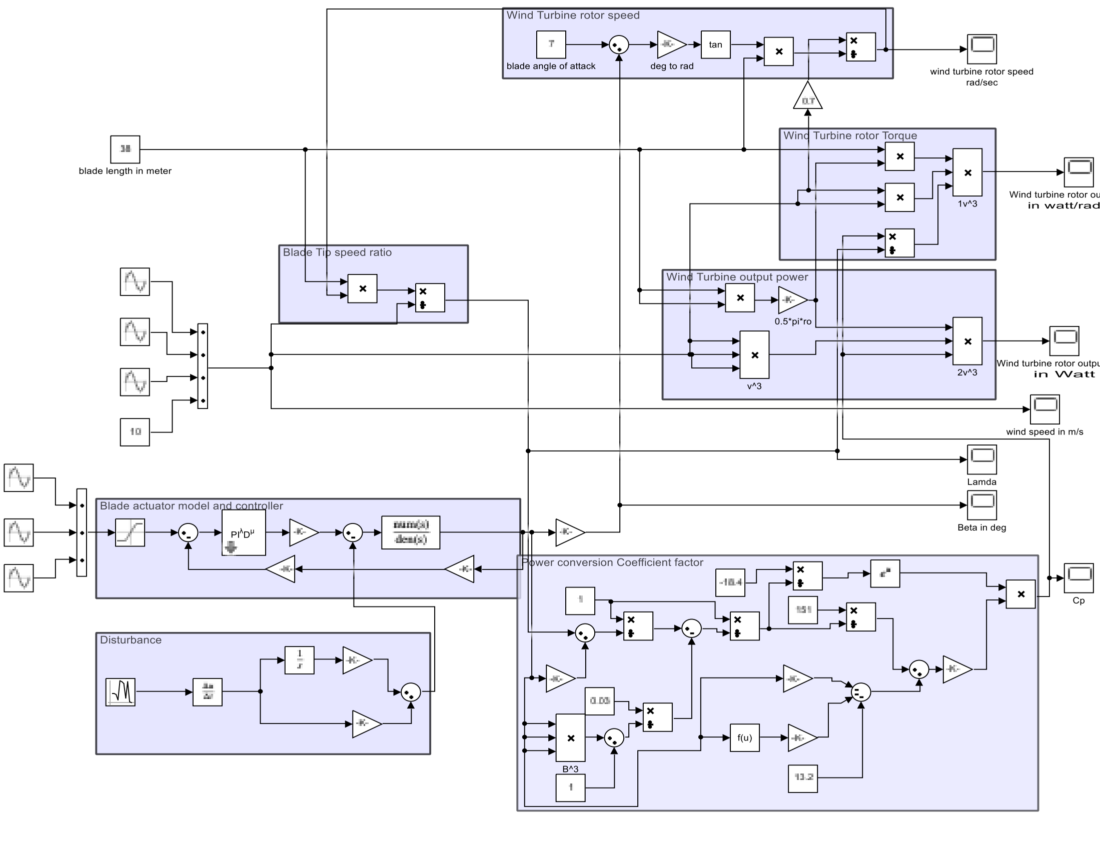

Figure 5.1 Complete System Diagram

5.2 Controller Performance for Different Reference Signals

5.2.1 Step Reference Input Tracking

When the wind speed is above rated the mechanical power and torque increase above rated value and the change of pitch angle limit excessive output power and torque turbine blade. Let's consider steady wind speed around the turbine blade and the system operates above rated wind speed. In this case, the mechanical power and torque are set at a rated value due to steady wind speed the power and torque have a constant value, and the turbine blade pitch angle sets at some degree to regulate the turbine output power and also reduce excessive torque around the blade. To measure the performance of the controllers in this study consider setting the pitch angle of the wind turbine blade at some constant degree, in this case, the pitch angle actuator control mechanism performances can be measured. To drive the blade pitch angle the directional control valve flow and spool position must be controlled to set the hydraulic cylinder piston at the desired position and it is proportional to the change of the pitch angle of the wind turbine blade. For this study the FOPID, GA-based PID, and GA-based FOPID are used, based on the performance measurement GA-FOPID has better performance than PID and FOPID, it provides a quick response for set point change of pitch angle with acceptable overshoot than PID controller. Generally, the quantitative comparisons between the control methods are summarized in the following table. From Table 5.1, one can observe that GA-FOPID gives shorter rise time, settling time, and smaller IAE than those of the PID and FOPID controller.

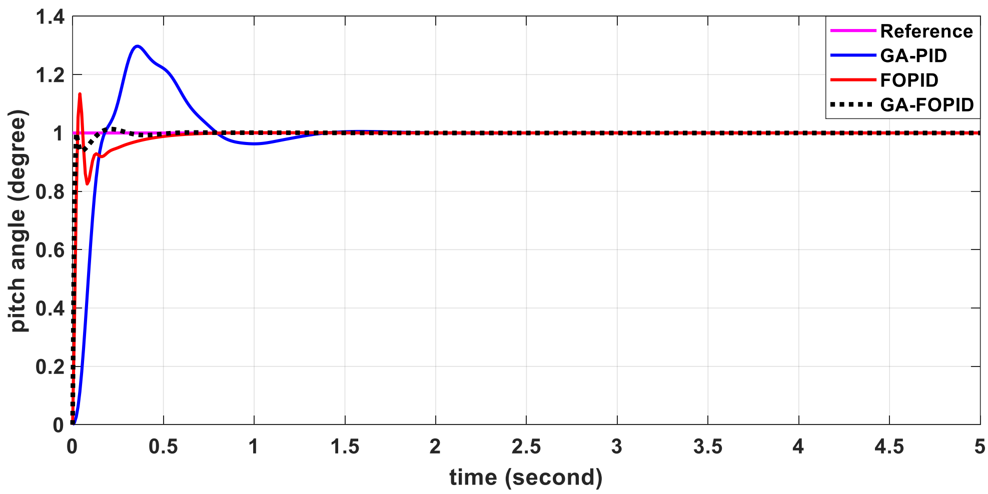

Figure 5.2 pitch angle responses for FOPID, GA-FOPID, and GA-PID for step reference signal

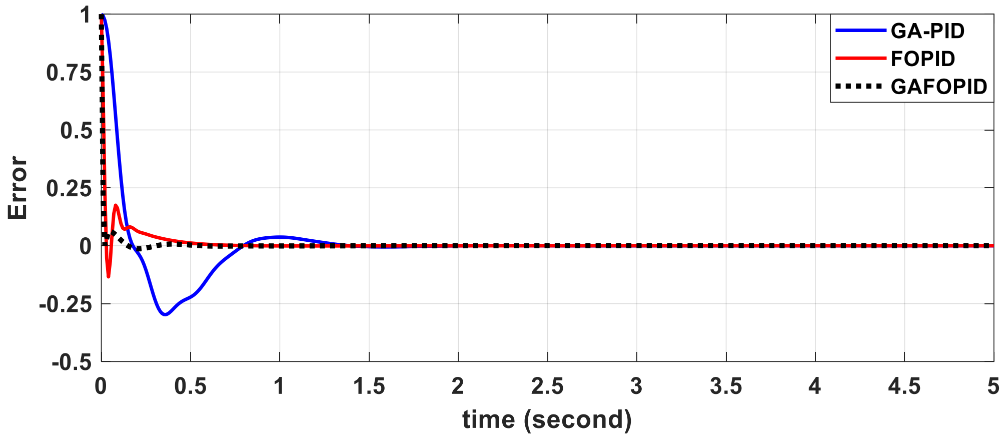

Figure 5.3 Step reference signal tracking error for GA-PID, FOPID, and GA-FOPID

Table 5.1 Controllers Tracking Performance Evaluation

Controllers	Performance measures			
	t_r (sec.)	t_s (sec.)	M_p (%)	IAE
GA-PID	0.1032	1.1887	29.74	0.1921
FOPID	0.0217	0.4165	13.427	0.0351
GA-FOPID	0.0139	0.1159	1.344	0.010

5.2.2 Sinusoidal Reference Input Tracking

By nature, wind speed is changing stochastically this stochastic change in wind speed affects the overall operation of the wind energy conversion system. When the wind speed varies stochastically and it has a value above the rated turbine blade pitch angle must be changed accordingly to set turbine power, torque, and rotor speed at the rated value and limit the mechanical overload on the system. To get the desired pitch angle the actuator must have good reference tracking ability. When the reference changes the proportional directional control valve drives the hydraulic cylinder piston accordingly to set the turbine blade at desired pitch angle. The performance of the controller was measured based on the IAE value. From figure 5.4, the value of the integral absolute error of the PID controller equals 5.167 and the FOPID without optimization has an IAE value of around 4.396 and the GA-based FOPID has an integral error of around 1.452. The FOPID has an approximately acceptable integral error value than GA-PID and the GA-FOPID has better error reduction performance and has an acceptable integral error than types of control techniques.

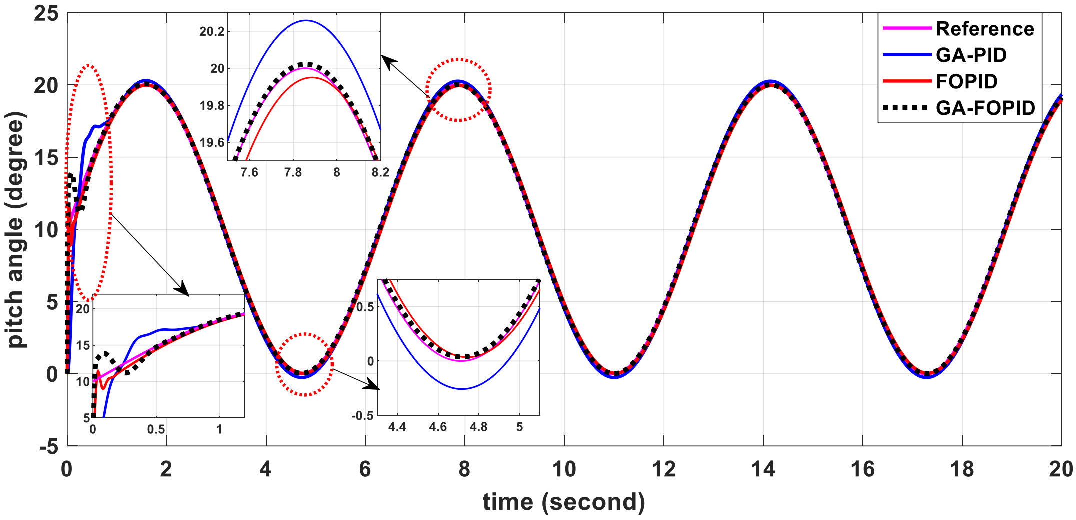

Figure 5.4 pitch angle responses for FOPID, GA-FOPID, and GA-PID for sinusoidal reference signal

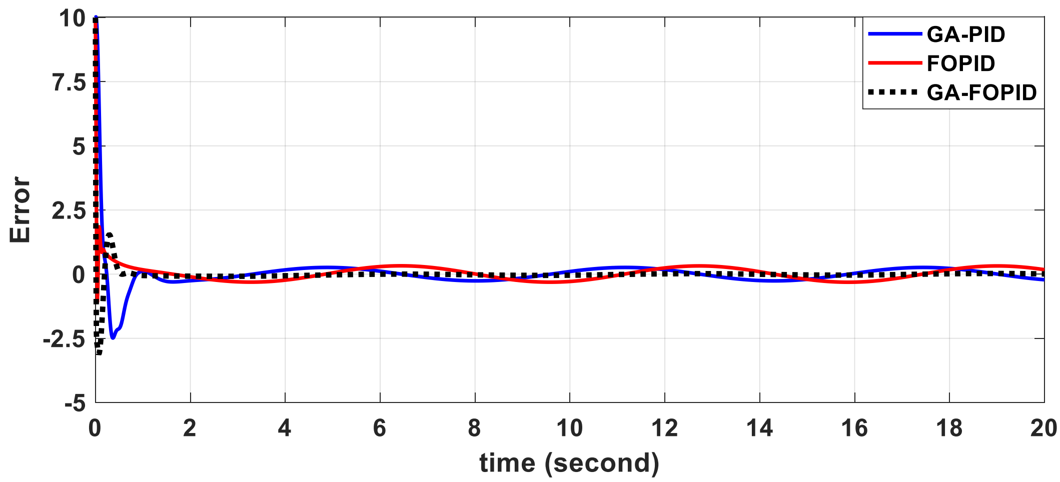

Figure 5.5 Sinusoidal reference signal tracking error for GA-PID, FOPID, and GA-FOPID

5.2.3 Stair Case Reference Input

Due to the effect of wind gusts, there may have a sudden change in wind speed around the wind turbine. The effects of the sudden change in wind speed are reduced by changing the turbine blade pitch angle. To measure the performance of the proposed control method staircase signal is used as the reference to show the sudden change in pitch angle due to a sudden change in wind speed above the rated value in both the opening and closing pitch. The performance of the controller was measured based on IAE.

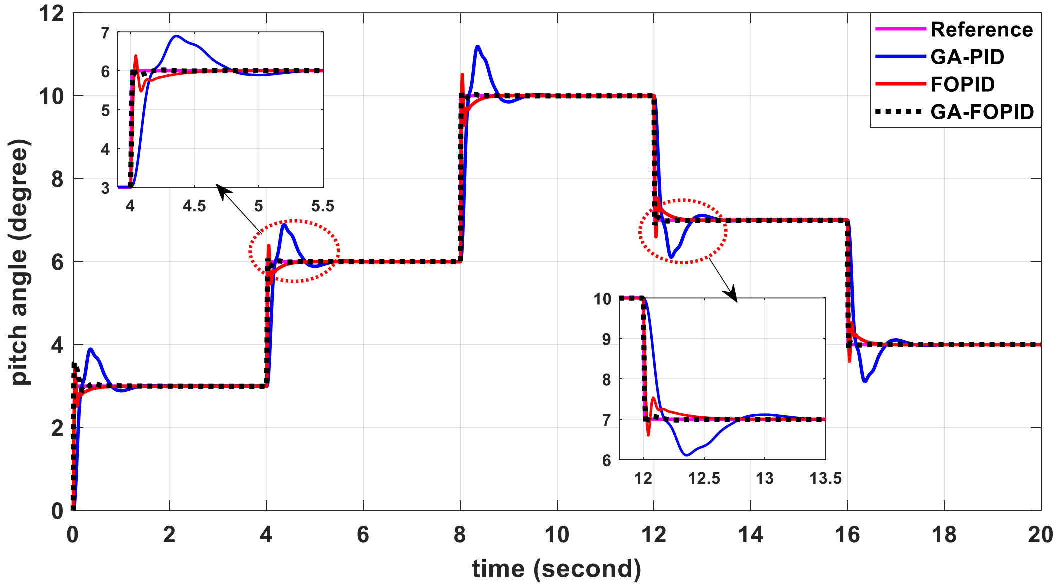

Figure 5.6 pitch angle responses for FOPID, GA-FOPID, and GA-PID for staircase reference signal

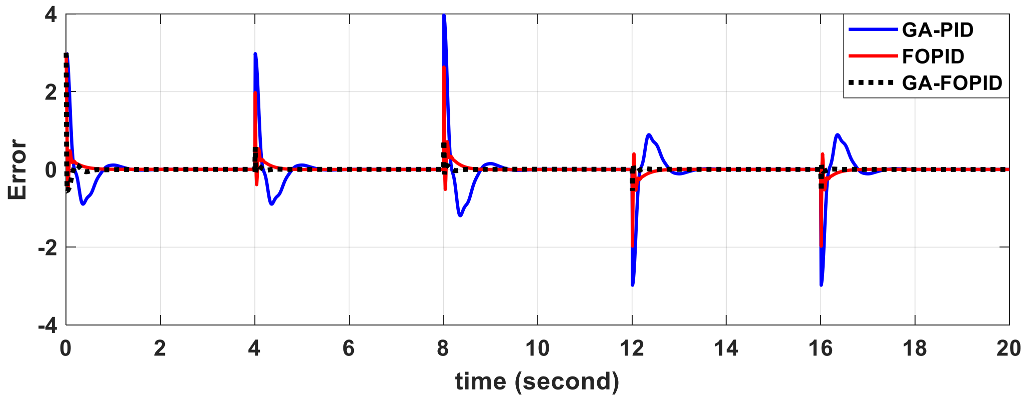

Figure 5.7 Staircase reference signal tracking error for GA-PID, FOPID, and GA-FOPID

From figure 5.6, the value of the integral absolute error of the PID controller equals 4.0 and the FOPID without optimization has an IAE value of around 0.6031 and the GA-based FOPID has an integral error of around 0.2506. Based on the value of IAE GA-FOPID has an acceptable value than the PID controller. From the IAE value, GA-FOPID reduces by 93.735% from GA-PID and by 58.448% from the FOPID controller. From figure 5.6, the PID controller introduces overshoot and undershoot during a sudden change in pitch angle therefore The GA-FOPID has a good response as compared with the PID and FOPID controllers.

5.3 Controller Performance under disturbance Load Torque

The turbulent nature of the wind, wind shear, and the wake effect at the root of the wind turbine blade all contribute to load torque in wind turbine pitching. It is unsteady and time-varying, and it harms the tracking performance of the hydraulic pitch control system. The effect of load torque varies depending on the pitch angle and wind speed around the turbine blade. If the wind speed is high and the turbine pitch angle is set around zero, the effect of load torque at the blade root increases, and if the pitch angle of the blade increases, the effect of load torque decreases due to the reduction of the attack angle of the turbine blade. Figure 5.8 shows the load torque added in the control system to measure the disturbance rejection performance of the controllers between 7 and 15sec by considering the maximum amplitude around 2500 NM.

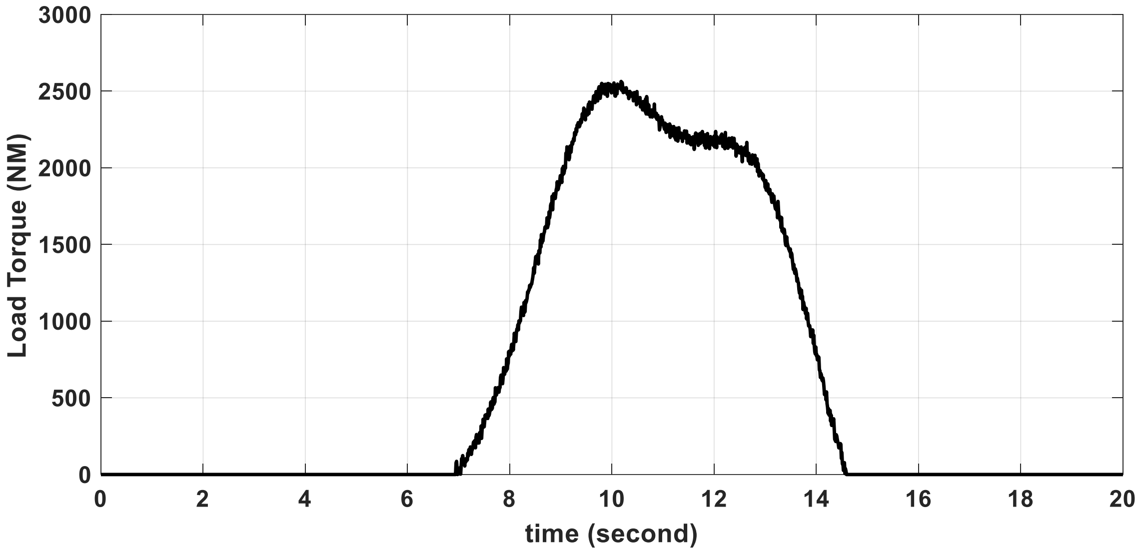

Figure 5.8 Disturbance load torque

Figure 5.9 depicts the step reference tracking response of the system when the dynamic disturbance load torque is added to it. When measuring the disturbance rejection performance of the hydraulic actuator based on the settling time and IAE value, GA-PID has around 1.188sec and 0.1926, FOPID has 0.4168sec and 0.04891, and GA-FOPID has 0.1160sec and 0.01099 settling time and IAE value when the system is subjected to the disturbance load torque. Figure 5.9 shows that due to the presence of the dynamic disturbance load torque, both control methods continue to track the given reference with some fluctuation. Even though the GA-FOPID has less fluctuation than the other controllers, as shown in the zoom portions of Figure 5.9.

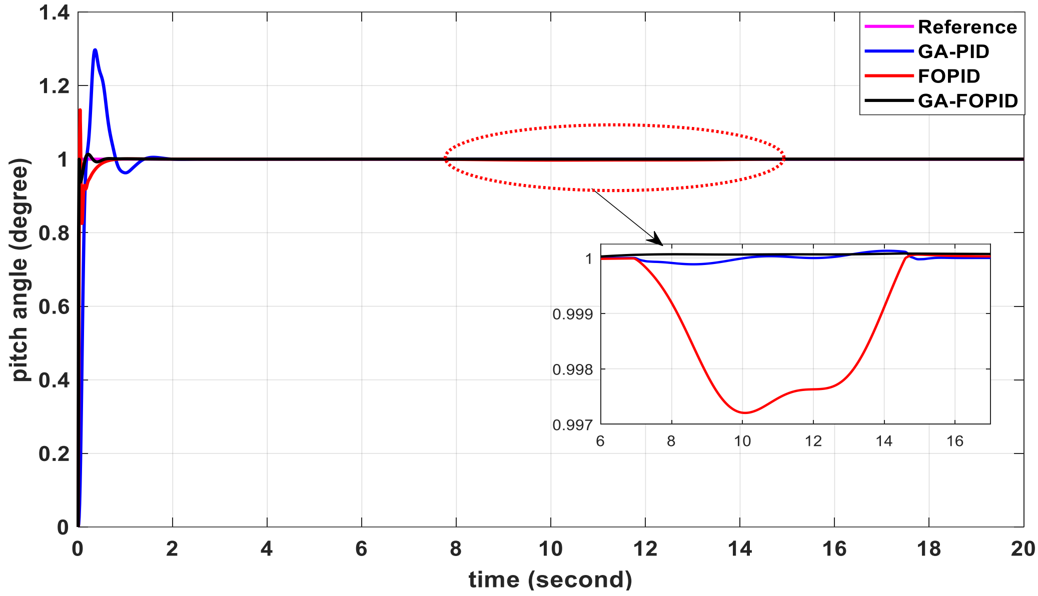

Figure 5.9 Step response for hydraulic actuator under the effect of load torque

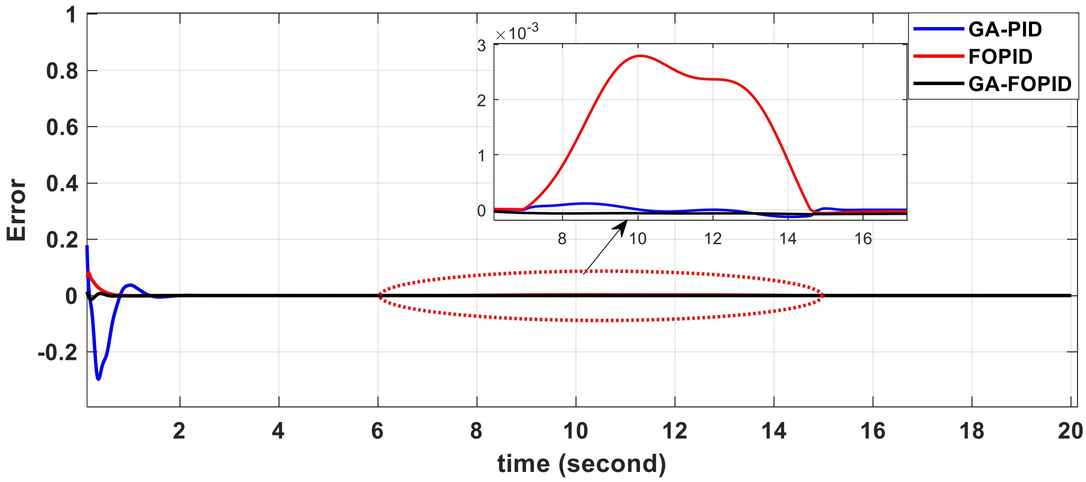

Figure 5.10 Tracking error response for step reference input under the effect of load torque

Table 5.2 shows the performance measure controllers based on the tracking performance of step tracking response by considering rise time, settling time, overshoot, and IAE of both controllers under the effect of the disturbance load torque. According to the comparison table, GA-FOPID has a lower performance measurement value than FOPID and GA-PID when the system is subjected to the disturbance load torque.

Table 5.2 Controllers Tracking Performance Evaluation under the effect of disturbance load torque

Controllers	Performance measures			
	t_r (sec.)	t_s (sec.)	M_p (%)	IAE
GA-PID	0.1032	1.1887	29.74	0.1926
FOPID	0.0217	0.4168	13.423	0.0489
GA-FOPID	0.0139	0.1159	1.344	0.0109

When comparing the performance of the controllers with and without the effect of disturbance load torque based on settling time and IAE value. When the performance of GA-FOPID with disturbance effect is considered, the settling time increases by 0.0862%, and the IAE value increases by 0.2596%. When the performance of FOPID is taken into account, the settling time increases by 0.0719%, and the IAE value increases by 28.235%. Finally, GA-PID has the same settling time with and without the effect of the disturbance, but the IAE value increases by 0.2596% when the disturbance effect is considered. According to the analysis, the effect of disturbance increases the value of settling time and IAE for both GA-FOPID and FOPID, but there is no change in settling time for the GA-PID controller.

5.4 Performance of Controlled Wind Turbine under Variable Wind Speed

When considering variable wind speed around the wind turbine at low wind speed, the wind turbine blade pitch angle is set around zero due to this the tip speed and the power coefficient have a maximum value which means the change of wind turbine blade pitch angle inversely affects the tip speed ratio and power coefficient. When the wind speed is above the rated value both mechanical power, mechanical torque, and rotor speed have the value above the rated due to this the system is put under the effect of mechanical overload. To reduce the effect of mechanical overload the turbine blade pitch must be increased and set the mechanical power, torque, and rotor speed set around the rated value. The above figure 5.11 shows the variable wind speed which varies between 1.5m/sec and 19m/sec to show the effect of pitch angle on the turbine dynamics.

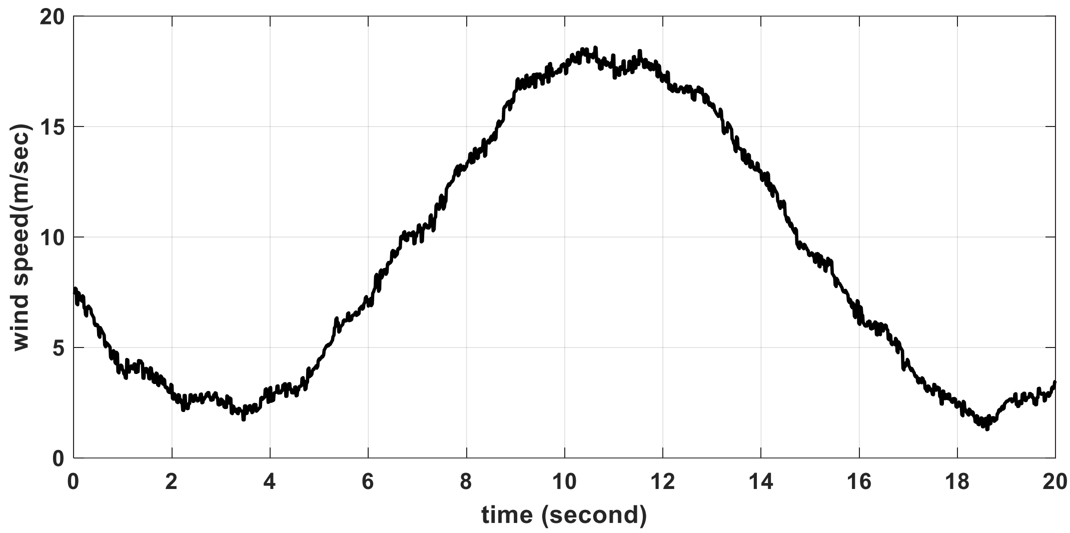

Figure 5.11 Continuous Variable wind speeds

If there is wind speed above the rated value of the turbine the pitch angle actuator changes the position of the hydraulic cylinder piston to limit the effect of mechanical overload on the system. From figure 5.12, the three control methods have different responses to changes in pitch angle for the continuous change of wind speed varying between 1.5-19m/sec. The GA-PID introduces overshoot and undershoots as compared with the other method which harms the mechanical component of the system and also leads to getting unstable power output when wind speed is above the rated value. The FOPID and GA-FOPID have more acceptable responses than the PID control method.

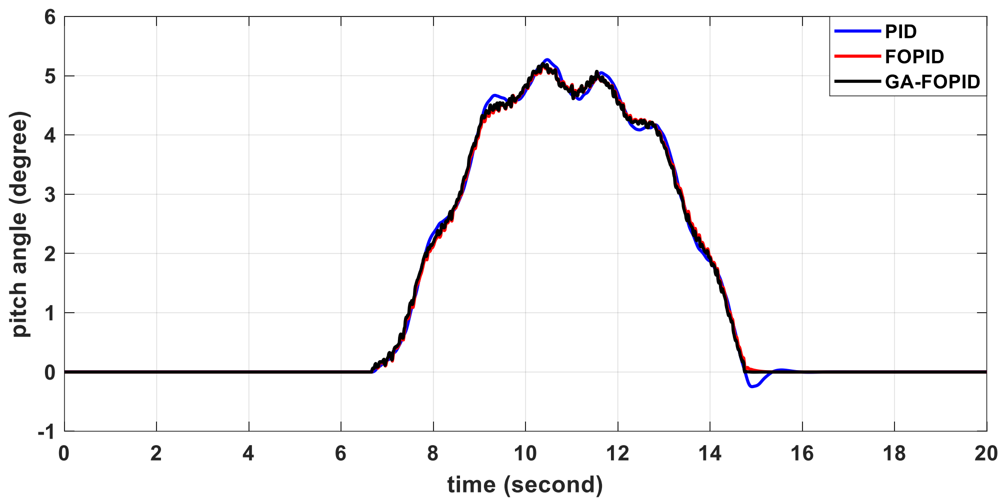

Figure 5.12 Pitch Angle Response for FOPID, GA-FOPID, and GA-PID for variable wind speed

Based on figure 5.12 around 2.5sec the wind speed is below the rated value of the turbine, the hydraulic cylinder piston shifts to the right, and the blade pitch angle is reduced to around 0^o to capture maximum power. When the time is around 10sec the wind speed reaches around 18.5m/sec and the turbine operates above the rated value to limit the power output the hydraulic cylinder piston shifts to the left the pitch angle is set to around 5^o and set the power at the rated value. The change of pitch angle is around 5^o and then considering the effect of twist angle the change of pitch angle reaches around 12^o.

From figure 5.13 when wind speed is below the rated value the tip speed ratio has a value of around 5.7, For this study consider three-bladed type horizontal axis wind turbines. Below-rated wind speed of around 2sec the tip speed has a high value because the pitch angle is set around zero degrees. To get optimal tip speed the pitch angle must be set around zero degrees because when the pitch angle is around zero the wind hits almost most of the turbine blade. When the wind speed is above the rated value increase in the pitch angle of the turbine blade reduces the value of tip speed. From figure 5.13 around 7sec, the wind speed has a higher value due to this the pitch angle of the blade increase. The increment of pitch angle reduces the rotor blade tip speed ratio value. It shows when wind speed is above the rated value small change in blade pitch angle highly affects the speed of the rotor at the blade tip.

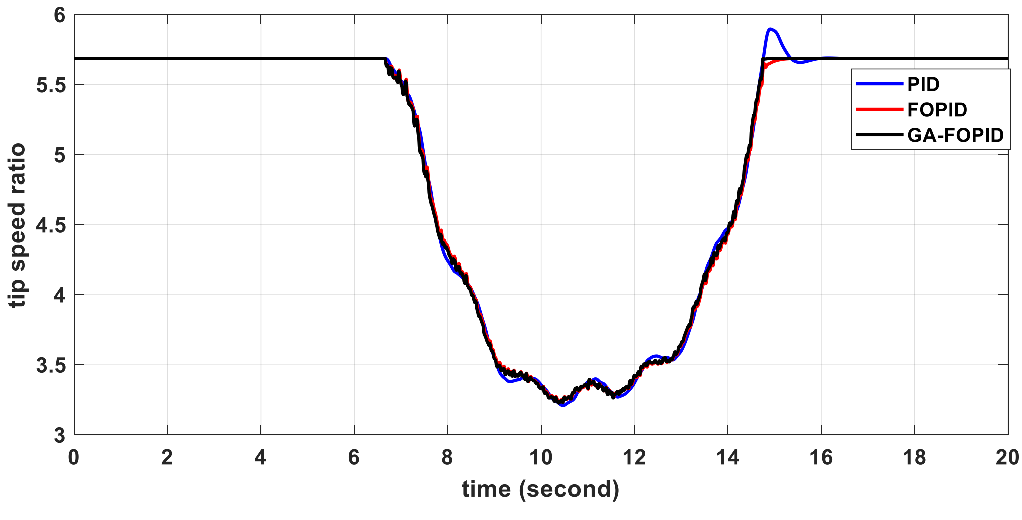

Figure 5.13 Tip Speed Response for FOPID, GA-FOPID, and GA-PID for variable wind speed

From figure 5.14 when the wind speed is below the rated value the turbine rotor rotates below the rated rotor speed. When the time is at 2sec the wind speed has a value below 3 m/sec and the rotor of the turbine rotor rotates below the rated value of around 0.4 rad/sec.

it shows when wind speed is below the rated value the change in wind speed and rotor speed is directly related. If the wind speed is above the rate the rotor speed increase causes the change of pitch angle of the blades and limits the rotor speed by changing the angle of attack of wind on the blade surface. High rotor speed causes a mechanical overload on the system. To reduce the effect of mechanical overload due to excessive wind speed around the blade the change of pitch angle of the turbine blade has a great effect.

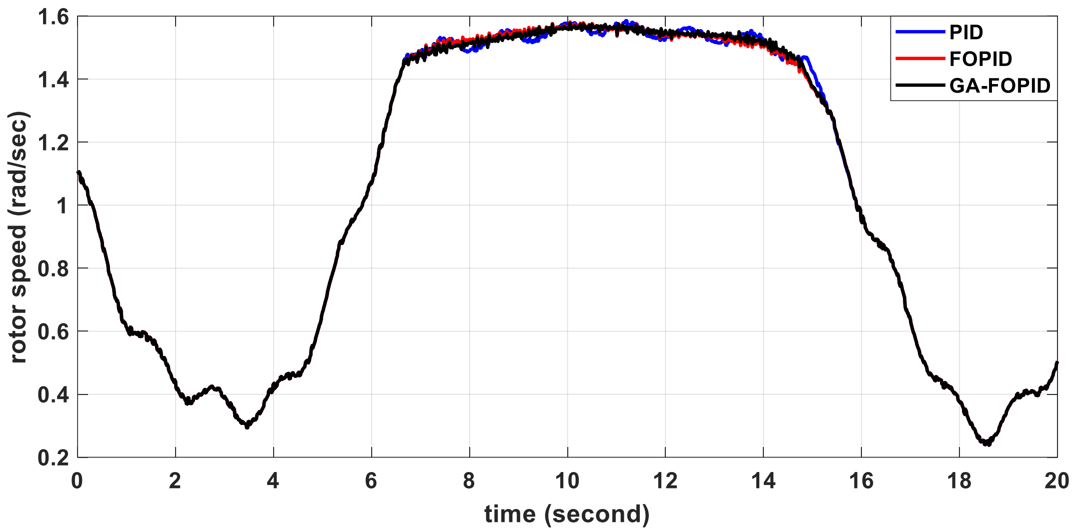

Figure 5.14 Rotor Speed Response for FOPID, GA-FOPID, and GA-PID for variable wind speed

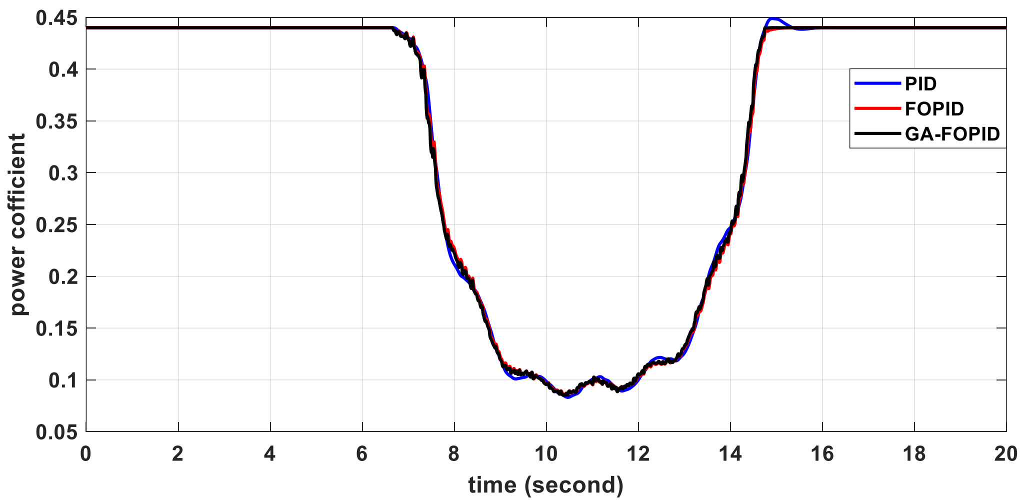

Figure 5.15 Power Coefficient Responses for FOPID, GA-FOPID, and GA-PID for variable wind speed

The power coefficient has a great role in power regulation, it has an inverse relation with blade pitch angle. When the wind speed is above the rated value the pitch angle of the blade increases which reduces the value of the power coefficient, it limits the output power of the system. From figure 5.15 at lower wind speed the power coefficient has a higher value when wind speed increases above the rated value the pitch angle of the blade increases which reduces the power coefficient.

The power obtained from wind turbines highly depends on wind speed, from figure 5.16 When the wind speed is below the rated turbine power output increase with wind speed this is because below the rated wind speed the turbine blade pitch angle is set around zero, in this case, the power coefficient has the higher value due to direct relation between power coefficient and blade turbine mechanical power the power coefficient has higher value turbine operates to capture maximum power from wind energy. When the wind speed is above the rated value the power output is regulated around the rated value due to the effect of the change of pitch angle on the power coefficient. When wind speed is above the rated value of the turbine From figure 5.12 the overshoot introduced due to the change of turbine blade pitch angle in GA-PID causes oscillation on the turbine mechanical power output it may cause stability problems in system power output, FOPID and GA-FOPID has good performances.

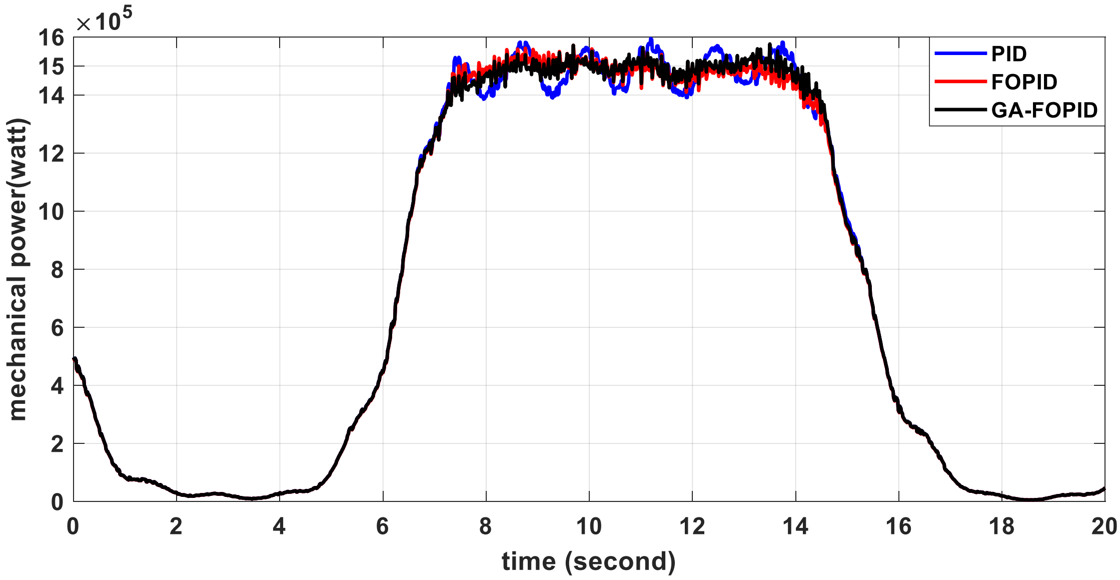

Figure 5.16 turbine mechanical power responses for FOPID, GA-FOPID, and GA-PID for variable wind speed

In complex wind energy conversion systems, there exists nonlinear relation between turbine aerodynamic torque and blade pitch angle. From figure 5.17 When wind speed is below the rated value Pitch angle changes have small effects on the force situation because below rated wind speed blade surface is almost perpendicular to the wind flow direction to capture maximum power. Whereas at higher wind speed the pitch angle is larger, and aerodynamic torque becomes more sensitive to pitch angle changes, which means dramatic force behavior could be caused by small changes in pitch angle.

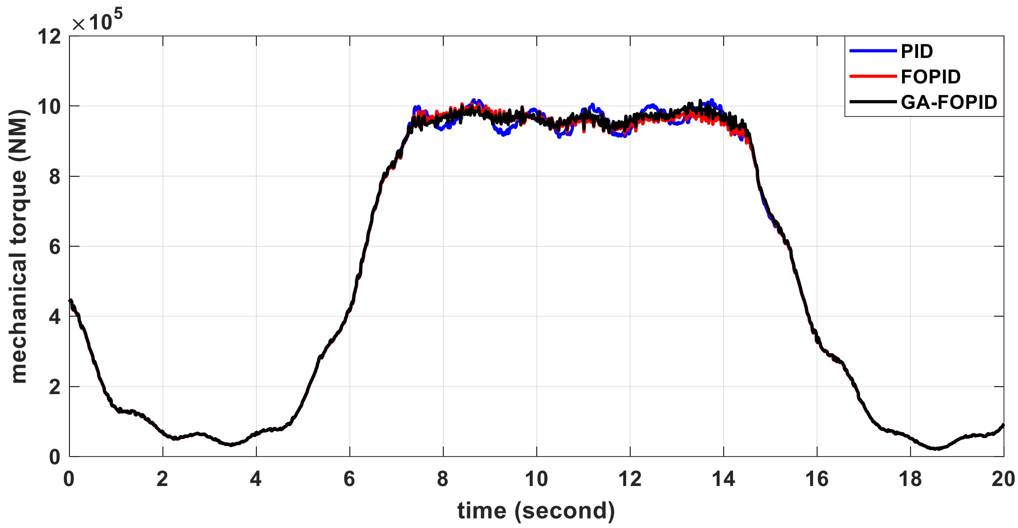

Figure 5.17 Turbine mechanical torque responses for FOPID, GA-FOPID, and GA-PID for variable wind speed

5.5 Discussion of The Result

From the above result and discussion, the hydraulic system tracking performance is measured based on different reference signals by considering the working environment of the system. The performance measure value for step reference input Based on Table 5.1 generalizes the step reference performance characteristics of the three controllers, when considering the performance of GA-FOPID reduces 95.48% overshoot from GA-PID and 89.99% from FOPID, it shows the performance of the proposed controller in reduction of the effect of overshoot. Also, GA-FOPID reduces 86.53% rise time from GA-PID and 35.94% from FOPID, settling time reduces 90.24% from GA-PID and 72.172% from FOPID, lastly, GA-FOPID reduces 94.794% IAE value from GA-PID and 71.50% from FOPID. From the above analysis, GA-FOPID has a good transient performance measure and a small IAE value than conventional PID.

For the sinusoidal reference signal the performance of the controllers was measured based on the IAE value, From the IAE value, GA-FOPID reduces the IAE value by 71.898% from GA-PID and also it reduce the IAE value by 66.96% from the FOPID controller. Also for the staircase reference signal, the performance of the controllers was measured using the IAE value, From the IAE value obtained GA-FOPID reduces the IAE value by 93.735% from GA-PID and it reduce the IAE value by 58.448% from the FOPID controller. From the performance of the controller's analysis GA-FOPID has a small IAE than the PID.

Load torque affects the system performance measurement in this case the performance of the controllers compares based on settling time, rise time, peak overshoot, and the IAE value. In FOPID and GA-FOPID controllers, the load torque disturbances increase the settling time and IAE value by some amount but in GA-PID the settling time has no change when the system operates with and without the effect of load torque but it has a change in the IAE value of the controller.

Table 5.3 Summary of the effect of blade Pitch angle change on wind turbine dynamics

Wind speed (m/sec.)	**2.8**	**13.39**	**18.4**	**6.3**	**1.68**
Pitch angle (degree)	0	2.19	5.15	0	0
Rotor speed (rad/sec)	0.5221	1.51	1.56	1.354	0.443
Tip speed	5.7	4.29	3.242	5.7	5.7
Power coefficient	0.44	0.2214	0.086	0.44	0.44
Mechanical power (watt)	27,000	1.47×10^{6}	1.5×10^{6}	315,000	5,054
Torque (NM)	705,90	967,700	950,0. 00	662,600	68,000

Lastly consider the performance of the controllers and the effect of pitch angle control on turbine tip speed, rotor speed, power coefficient, mechanical power, and mechanical torque of the system based on different ranges of wind speed. From the summary in table 5.3 when wind speed is below rated the pitch angle is set around zero due to this the turbine tip speed and power coefficient have a higher value. But the rotor speed, mechanical torque, and mechanical power increase with wind speed. When wind speed is above the rated value the pitch angle increase to regulate the turbine power and torque around the rated value. The pitch angle increases the power coefficient of the turbine reduce to limit the power output at the rated value, the pitch angle change also affects the rotor speed above the rated wind speed the rotor speed is set around the rated value due to the effect of pitch angle.

CHAPTER SIX

CONCLUSION AND RECOMMENDATION

Conclusion

The wind energy conversion system is one of the methods used to get electric energy from wind energy without the effect on the environment. The wind turbine is the system that converts the variable wind speed to useful electrical energy based on the combination of different components and control systems to improve its performance. The turbine system is one of the systems that convert variable wind speed to mechanical energy. The variation in wind speed affects the output power and the rotational speed of the wind turbine. When the wind speed varies above the rated value correspondingly power and rotational speed increase accordingly. To limit the variation of power and rotational speed and also to reduce mechanical overload the turbine blade angle must vary along their longitudinal axis. From different pitch driving mechanisms, the hydraulic actuator is one of the methods considered in this study. GA-PID, FOPID, and GA-FOPID are the controllers used to control the hydraulic system. The controller adjusts the position of the directional control valve spool to control the amount of flow and the direction of flow of fluid to the hydraulic piston, which is used to adjust the pitch angle of the turbine using a slider crank mechanism that fixes at the root of the turbine blade. From the analysis of step response, the PID has a 29.74% overshoot and 1.188 settling times, FOPID has a 13.42% overshoot and 0.41 settling time and the GA-FOPID has a 1.344% and 0.115 overshoot and settling time. From the three control mechanism, GA-FOPID has good tracking performance than the other control mechanism. Lastly consider the effect of the actuator on the measurable output of the turbine dynamics. During analysis consider the effect of the driving mechanism on rotor speed, tip speed ratio, power coefficient, turbine power, and torque based on the relationship between the turbine component and blade pitch angle change. During analysis consider the random variation of wind speed between 1.5 m/sec to 19m/sec. From the simulation result, the FOPID and GA-FOPID have good response than the PID controller. Based on the system response if the wind speed is below the rated value the pitch angle of the turbine is set around 0^0 in this case the tip speed ratio and power coefficient have the value around 5.7 and 0.44 the mechanical power and the rotor speed have the value below the rated. When the wind speed is set above the rated value the pitch angle of the wind turbine blade starts to increase to limit the mechanical power and rotor speed. In this case, the tip speed and the power coefficient of the turbine start to decrease due to the effect of the wind turbine blade pitch angle. The mechanical power is highly affected by the power coefficient and the mechanical torque of the turbine depends on the mechanical power and the rotor angular speed when the wind speed is below the rated value the pitch angle has less effect on the mechanical torque but when the wind speed above the rated value small change of pitch angle highly affect the mechanical torque of wind turbine.

Recommendation

This study considers improving the set point tracking performance of the hydraulic pitch actuator based on PID and FOPID with GA optimization. The future study recommends considering the effect of leakage on the hydraulic pitch actuator system and the techniques used for fault detection mechanisms. And also this study can be further improved by considering an advanced control technique such as a sliding mode, model predictive control, etc. to improve the performance of the hydraulic system.

Research fund Acknowledgement

This research thesis was funded by Adama Science and Technology University under the grant number **ASTU/SM-R/566/22**, Adama, Ethiopia.

REFERENCE

Apata, O., & Oyedokun, D. T. O. (2020a). An overview of control techniques for wind turbine systems. *Scientific African*, *10*, e00566. https://doi.org/10.1016/j.sciaf.2020.e00566

Azevedo, G. (2009). *Modeling of a Variable Speed Wind Turbine with a Permanent Magnet Synchronous Generator*. *ISlE*, 734–739.

Azevedo, G. (2013). *Modeling of a Variable Speed Wind Turbine with a Permanent Magnet Synchronous Generator V2*. *ISlE*, 734–739. http://inpressco.com/wp-content/uploads/2014/02/Paper78421-426.pdf

Baburajan, S., & Ismail, A. (2017). Pitch Control of Wind Turbine through PID, Fuzzy and an Adaptive Fuzzy-PID Controller System : *International Research Journal of Engineering and Technology(IRJET)*, *4*(9), 669–675. https://irjet.net/archives/V4/i9/IRJET-V4I9115.pdf

Borg, M., & Collu, M. (2012). *Offshore Floating Vertical Axis Wind Turbines : Advantages, Disadvantages and Dynamics Modeling State of the Art*. *September*. https://doi.org/10.3940/rina.mre.2012.05

Burton, T., Jenkins, N., Sharpe, D., & Bossanyi, E. (2011). Conceptual Design of Horizontal Axis Wind Turbines. In *Wind Energy Handbook*. https://doi.org/10.1002/9781119992714.ch6

Chipipop, B., & Calculus, A. F. (2019). Designing of Fractional Order PID Controller for Unstable Fractional Order System. *2019 Joint International Conference on Digital Arts, Media, and Technology with ECTI Northern Section Conference on Electrical, Electronics, Computer, and Telecommunications Engineering (ECTI DAMT-NCON)*, 81–84.

Choudhary, S. K. (2015). *Stability and Performance Analysis of Fractional Order Control Systems*. *November 2014*. https://doi.org/10.5281/zenodo.2590916

Civelek, Z., Lüy, M., Çam, E., & Barışçı, N. (2015). *Control of Pitch Angle of Wind Turbine by Fuzzy Pid Controller Control of Pitch Angle of Wind Turbine by Fuzzy Pid Controller*. *8587*(November), 0–9. https://doi.org/10.1080/10798587.2015.1095417

Dong, G., Qin, J., Li, Z., & Yang, X. (2022). An Inverse Method for Wind Turbine Blade Design with Given Distributions of Load Coefficients. *Wind*, *2*(1), 175–191. https://doi.org/10.3390/wind2010010

Dou, Z. L., Cheng, M. Z., Ling, Z. B., & Cai, X. (2010). An adjustable pitch control system in a large wind turbine based on a fuzzy-PID controller. *SPEEDAM 2010 - International Symposium on Power Electronics, Electrical Drives, Automation and Motion*, 391–395. https://doi.org/10.1109/SPEEDAM.2010.5542220

Feng, W., Deng, Y., Li, H., Chen, D., & Li, F. (2021). Design of novel hybrid control for permanent magnet synchronous generator–based wind energy conversion system. *JVC/Journal of Vibration and Control*, *September 2020*. https://doi.org/10.1177/10775463211010533

Gambier, A. (2021). *Pitch Control of Three Bladed Large Wind Energy Converters — A Review*. 1–24.

Gambier, A., & Yunazwin Nazaruddin, Y. (2018). Nonlinear PID Control for Pitch Systems of Large Wind Energy Converters. *2018 IEEE Conference on Control Technology and Applications, CCTA 2018*, 996–1001. https://doi.org/10.1109/CCTA.2018.8511531

George, T., & Ganesan, V. (2020). *Optimal tuning of PID controller in time delay system : a review on various optimization techniques*. 1–28.

Gowdar, R. D., & Mallikarjune Gowda, M. C. (2016). Reasons for wind turbine generator failures: a multi-criteria approach for sustainable power production. *Renewables: Wind, Water, and Solar*, *3*(1), 1–8. https://doi.org/10.1186/s40807-016-0029-1

Gu, X., & Hui, J. (2008). *Study on a Novel Hydraulic Variable-Pitch System of Wind Turbine*. 3–6.

Hamamci, S. E. (2008). Stabilization using fractional-order PI and PID controllers. *Nonlinear Dynamics*, *51*(1–2), 329–343. https://doi.org/10.1007/s11071-007-9214-5

Hui, P., Ping, W., & Weihua, L. I. (2019). Model-Based Fractional Order PID Controller Design and Simulation of Pressure Swing Adsorption. *2019 Chinese Control Conference (CCC)*, 2880–2883.

Islam, M. A., Hasanuzzaman, M., Rahim, N. A., Nahar, A., & Hosenuzzaman, M. (2014). Global renewable energy-based electricity generation and smart grid system for energy security. *Scientific World Journal*, *2014*. https://doi.org/10.1155/2014/197136

J.Jebakumar, K.Mishra, & B.MISHRA. (2014). Controller Selection and Sensitivity Check on the Basic of Performance Index Calculation. *International Journal of Electrical, Electronics and Data Communication*, *2*(1), 91–93.

Johnson, D. A., Gu, M., & Gaunt, B. (2016). Wind Turbine Performance in Controlled Conditions: BEM Modeling and Comparison with Experimental Results. *International Journal of Rotating Machinery*, *2016*. https://doi.org/10.1155/2016/5460823

Kalpaktsoglou, D., Pouros, S., & Kleidis, K. (2019). *Improving the efficiency of a wind* *turbine using Thyristor Switched Series Capacitors-A simulation study Improving the efficiency of a wind turbine using Thyristor Switched Series Capacitors- A simulation study*. *May*.

Karlborg, J., & Sten, E. (2021). *Braking with a Directional Control Valve in a Hydraulic Open-Loop Transmission*.

Lasheen, A., Saad, M. S., Emara, H. M., & Elshafei, A. L. (2016). Explicit model predictive control with time-varying constraints for collective pitching in large wind turbines. *IECON Proceedings (Industrial Electronics Conference)*, 4121–4126. https://doi.org/10.1109/IECON.2016.7793552

Lee, C. T., & Moon, B. Y. (2011). The dynamic design of hydraulic pressure control valve of active suspension system using experimental method. *Proceedings of the 28th International Symposium on Automation and Robotics in Construction, ISARC 2011*, 1434–1439. https://doi.org/10.22260/isarc2011/0273

Lei, J. B., Wang, X. Y., Xu, Z. P., Luo, Y. X., & Pi, Y. J. (2010). Position control for asymmetrical hydraulic cylinder system using a single on/off valve. *Journal of Shanghai Jiaotong University (Science)*, *15*(6), 651–656. https://doi.org/10.1007/s12204-010-1063-6

Li, K., Gao, Q., Gong, J., & Hou, Y. (2015). *Modeling and Simulation of Electro-hydraulic Servo System of a Certain Weapon Barrel for Balancing and Positioning*. 3397–3401.

Manyonge, A. W., & Ochieng, P. (2014). *Mathematical Analysis of Tip Speed Ratio of a Wind Turbine and its Effects on Power Coefficient Mathematical analysis of tip speed ratio of a wind turbine and its effects on power coefficient*. *January*. https://doi.org/10.26708/IJMSC.2014.1.4.07

Meenu, P. V. (2019). *Power Regulation and Pitch Control of Wind Turbines using Actuator Fault Tolerant Adaptive Control*. *8*(05), 527–531.

Melício, R., Mendes, V. M. F., & Catalão, J. P. S. (2010). *Power converter topologies for wind energy conversion systems : Integrated modeling , control strategy, and performance simulation*. *35*. https://doi.org/10.1016/j.renene.2010.03.009

Menezes, N., Araújo, A. M., & Jos, E. (2018). *A review on wind turbine control and its associated methods*. *174*, 945–953. https://doi.org/10.1016/j.jclepro.2017.10.297

Numerical modeling of the hydraulic blade pitch actuator in a spar-type floating wind turbine.pdf. (n.d.).

Olume, W. I. N. D. E. N. V, Kong, Y., & Wang, Z. (2007). *Modelling and Analysing the Hydraulic Variable-pitch Mechanism for a Variable-speed Wind Turbine*. 341–352.

Owusu, P. A., & Asumadu-Sarkodie, S. (2016). A review of renewable energy sources, sustainability issues, and climate change mitigation. *Cogent Engineering*, *3*(1). https://doi.org/10.1080/23311916.2016.1167990

Pelin, R. I., Barsănescu, P. D., & Tiţa, I. (2018). Hydraulic systems used for pitch control of wind turbines: A literature overview. *IOP Conference Series: Materials Science and Engineering*, *444*(4). https://doi.org/10.1088/1757-899X/444/4/042013

Phan, V. Du, Vo, C. P., Dao, H. V., & Ahn, K. K. (2021). Robust Fault-Tolerant Control of an Electro-Hydraulic Actuator with a Novel Nonlinear Unknown Input Observer. *IEEE Access*, *9*, 30750–30760. https://doi.org/10.1109/ACCESS.2021.3059947

Qi, K. (2014). Research on variable pitch wind turbine control system. *Asia-Pacific Power and Energy Engineering Conference, APPEEC*, *2015-March*(March), 3–6. https://doi.org/10.1109/APPEEC.2014.7066117

Rashid, M. T., & Halihal, A. F. (2019). *Design of pitch angle controller for wind turbine based on pi neuro-fuzzy model*. *July*, 1664–1670. https://doi.org/10.11591/ijeecs.v15.i3.pp1664-1670

REN21, R. E. P. N. for the 21st C. (2009). *Renewables Global Status Report 2009*. 32.

Rhouma, A., Hafsi, S., & Laabidi, K. (2021). *Stabilizing and Robust Fractional PID Controller Synthesis for Uncertain First-Order plus Time-Delay Systems*. *2021*.

Rommel, D. P., Di Maio, D., & Tinga, T. (2020). Calculating wind turbine component loads for improved life prediction. *Renewable Energy*, *146*, 223–241. https://doi.org/10.1016/j.renene.2019.06.131

Ruderman, M. (2017). Full- and reduced-order model of hydraulic cylinder for motion control. *Proceedings IECON 2017 - 43rd Annual Conference of the IEEE Industrial Electronics Society*, *2017-Janua*(1), 7275–7280. https://doi.org/10.1109/IECON.2017.8217274

Sahib, M., & Nayl, T. (2019). A New Pitch Angle Control Method of Wind Turbine Generators Based on Feedforward Wind Speed Information. *E3S Web of Conferences*, *122*. https://doi.org/10.1051/e3sconf/201912204001

Sahoo, S., Subudhi, B., & Panda, G. (2019). *Torque and pitch angle control of a wind turbine using multiple adaptive neuro-fuzzy control*. https://doi.org/10.1177/0309524X19849825

Shutnan, W. A. (2018). *Artificial Immune system based Optimal Fractional Order PID Control Scheme for Path Tracking of Robot manipulator*. 19–24.

Sohoni, V., Gupta, S. C., & Nema, R. K. (2016). A Critical Review on Wind Turbine Power

Curve Modelling Techniques and Their Applications in Wind Based Energy Systems. *Journal of Energy*, *2016*(region 4), 1–18. https://doi.org/10.1155/2016/8519785

Studies, C., Buildings, G., & Sayigh, A. (2013). Sustainability, Energy, and Architecture. In *Sustainability, Energy, and Architecture*. https://doi.org/10.1016/c2011-0-07553-1

Sunyoto, A., Wenehenubun, F., & Sutanto, H. (2013). *The Effect of Number of Blades on the Performance of H-Darrieus type Wind Turbine*. 192–196.

Syed Hussien, S. Y., Jaafar, H. I., Ghazali, R., & Abdul Razif, N. R. (2015). The effects of auto-tuned method in PID and PD control scheme for gantry crane system. *International Journal of Soft Computing and Engineering (IJSCE)*, *4*(6), 121–125. http://eprints.utem.edu.my/14047/1/%5B1%5D_F2492014615.pdf

Tan, C., & Wang, H. H. (2013). A review on pitch angle control strategy of variable pitch wind turbines. *Advanced Materials Research*, *772*, 744–748. https://doi.org/10.4028/www.scientific.net/AMR.772.744

Teixeira, M. C. M., Assunçãno, E., & Covacic, M. R. (2007). Proportional controllers: Direct method for stability analysis and MATLAB implementation. *IEEE Transactions on Education*, *50*(1), 74–78. https://doi.org/10.1109/TE.2006.888903

Topologies, G. (2013). *A Review on Wind Turbine*. 625–629.

Wang, C., & Chiang, M. (2016). *A Novel Pitch Control System of a Large Wind Turbine Using Two-Degree-of-Freedom Motion Control with Feedback Linearization Control*. https://doi.org/10.3390/en9100791

West, C., Montazeri, A., Monk, S. D., & Taylor, C. J. (2016). A genetic algorithm approach for parameter optimization of a 7DOF robotic manipulator. *IFAC-PapersOnLine*, *49*(12), 1261–1266. https://doi.org/10.1016/j.ifacol.2016.07.688

Wu, F. B., Yang, B., & Ye, J. L. (2019). Grid-scale energy storage systems and applications. In *Grid-Scale Energy Storage Systems and Applications*. https://doi.org/10.1016/C2017-0-00957-6

Xu, B. (2018). *Modeling and Experimental Validation of the Time Delay in a Pilot Operated Proportional Directional Valve*. *6*, 30355–30369. https://doi.org/10.1109/ACCESS.2018.2844164

Xue, Y., & Tai, N. (2012). System frequency regulation in doubly fed induction generators. *International Journal of Electrical Power and Energy Systems*, *43*(1), 977–983. https://doi.org/10.1016/j.ijepes.2012.05.039

Yadav, A., & Appan, A. (2016). Steady-state analysis of Electronic Load Controller for a three-phase alternator. *12th IEEE International Conference Electronics, Energy,* *Environment, Communication, Computer, Control: (E3-C3), INDICON 2015*, *iv*. https://doi.org/10.1109/INDICON.2015.7443654

Yang, K. (2020). Geometry design optimization of a wind turbine blade considering effects on aerodynamic performance by linearization. *Energies*, *13*(9). https://doi.org/10.3390/en13092320

Zhang, J., Cheng, M., Chen, Z., & Fu, X. (2008). Pitch Angle Control for Variable Speed Wind Turbines Jianzhong Zhang, Ming Cheng, Zhe Chen, Xiaofan Fu Abstract--Pitch. *DRPT2008 6-9 April 2008 Nanjing China*, *April*, 2691–2696.

Zhang, J., Wang, D., Xu, B., Lu, Z., Gan, M., & Su, Q. (2018). Modeling and experimental validation of the time delay in a pilot-operated proportional directional valve. *IEEE Access*, *6*, 30355–30369. https://doi.org/10.1109/ACCESS.2018.2844164

Zhou, F., & Liu, J. (2018). Pitch Controller Design of Wind Turbine Based on Nonlinear PI/PD Control. *Shock and Vibration*, *2018*. https://doi.org/10.1155/2018/7859510

Zhu, Y., & Jin, B. (2016). Analysis and modeling of a proportional directional valve with a nonlinear solenoid. *Journal of the Brazilian Society of Mechanical Sciences and Engineering*, *38*(2), 507–514. https://doi.org/10.1007/s40430-015-0464-8

Zhu, Y., Li, G., Tang, S., Jiang, W., Qian, P., Zheng, Z., & Zheng, Z. (2021). Instability Condition Derivation for Hydraulic AGC System under Pressure Closed-Loop Control. *Shock and Vibration*, *2021*. https://doi.org/10.1155/2021/6618525

Appendix I

GA Simulink model optimization

```
%GA-PID for Simulink
function New_closed_loop_model_2_GA
clear all
rng default
options= optimoptions('ga','PlotFcn',@gaplotbestf);
options.PopulationSize= 20;
options.MaxGenerations= 50;  % Increase value if needed
nvar= 5; % Number of parameters
LB= [0.000093 0.00001 0 0.000001 0];
UB= [25 10 2 10 2];
[x,fval]=ga(@EvalObj,nvar,[],[],[],[],LB,UB,[],options)
%%
% Measures a performance index from the Simulink model
function obj= EvalObj(x)
% Updates the values of Kp, Ki, and Kd in Simulink model workspace
simulink_model= 'wind_turbine_aerodynamics_fopid11';
load_system(simulink_model);
gains= get_param(simulink_model,'modelworkspace');
gains.assignin('kpff', x(1));
gains.assignin('kiff', x(2));
gains.assignin('laff', x(3));
gains.assignin('kdff', x(4));
gains.assignin('muff', x(5));
% Simulates the Simulink model to get the outputs
simOut= sim(simulink_model,'SaveOutput','on');
% Retrieves time t and error e
t= simOut.find('t');
e= simOut.find('e');

% Calculate a performance index
n= length(e);
```

```
ae= abs(e);
obj= 0;
for i= 2:n
    stepsize= t(i)-t(i-1);
obj= obj+0.5*stepsize*(ae(i-1)+ae(i)); % IAE
end
```

Appendix II

Power coefficient versus tip speed graph

```
% Wind turbine
% Definition of parameters
% beta is the pitch angle
% lambda is the tip ratio
% Input parameters: r, vw, beta, ro
vw=[10:0.001:100];
beta=[0 4 8 12 16];
ro=1;
%End Inputs
for k=1:5
wr=2*pi*n/60;
lambda= r*wr./vw;
% Calculation of lambda_k
lambda_k=1./((1./(lambda+0.08*beta(k)))-(0.03/((beta(k))^3+1)));
% Calculation of power coefficient cp
cp=0.5176*(116./lambda_k-0.8*beta(k)-5).*exp(-21./lambda_k)+0.0068*lambda;
% Calculation of power
p=0.5*pi*ro*r^2.*cp.*vw.^3;
% Result
figure (1)
plot(vw,p), grid on, hold on,
figure (2)
plot(lambda,cp), grid on, hold on,
```

```
legend('Beta=0','Beta=4','Beta=8','Beta=12','Beta=16')
xlabel('tip Speed')
ylabel('Cp')
xlabel('wind speed')
ylabel('mechanical power')
end
```